



# The preparation and evaluation of core-shell magnetic dummy-template molecularly imprinted polymers for preliminary recognition of the low-mass polybrominated diphenyl ethers from aqueous solutions

Mariusz Marć<sup>a,\*</sup>, Piotr Paweł Wiczorek<sup>b</sup>

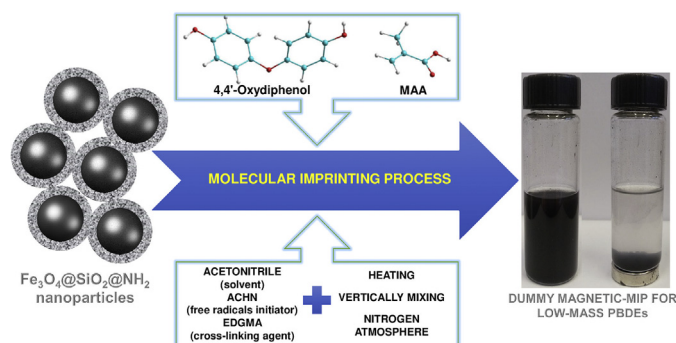
<sup>a</sup> Department of Analytical Chemistry, Faculty of Chemistry, Gdansk University of Technology, Gdansk, Poland

<sup>b</sup> Department of Analytical and Ecological Chemistry, Faculty of Chemistry, Opole University, Opole, Poland

## HIGHLIGHTS

- The preparation process of core-shell magnetic DMIP for low-mass PBDEs was described.
- The 4,4-Dihydroxydiphenyl ether was used as a dummy-template of low-mass PBDEs for magnetic MIP.
- The morphological structure and binding abilities of prepared magnetic DMIP were investigated.
- Synthesised magnetic DMIP shows sufficient specific recognition to low-mass PBDEs.
- The application potential of prepared magnetic DMIP for targeted analytes in water samples was studied.

## GRAPHICAL ABSTRACT



## ARTICLE INFO

### Article history:

Received 12 February 2020

Received in revised form 20 March 2020

Accepted 22 March 2020

Available online 25 March 2020

Editor: Thomas Kevin V

### Keywords:

Molecularly imprinted polymers  
 $\text{Fe}_3\text{O}_4$  nanopowder  
 Low-mass PBDEs  
 Aqueous solutions  
 4,4'-Dihydroxydiphenyl ether  
 Gas chromatography

## ABSTRACT

The design, preparation process, binding abilities, morphological characteristic and prospective field of application of dummy-template magnetic molecularly imprinted polymer (DMMIP) for preliminary recognition of the selected low-mass polybrominated diphenyl ethers (PBDE-47 and PBDE-99) from aquatic environment were investigated. The surface of iron oxide ( $\text{Fe}_3\text{O}_4$ ) nanopowder (50–100 nm particles size) was modified with tetraethoxysilane and next prepared  $\text{Fe}_3\text{O}_4@SiO_2$  particles were dispersed in anhydrous toluene functionalized by (3-aminopropyl)triethoxysilane. Finally, MIPs' thin film layer on the surface of  $\text{Fe}_3\text{O}_4@SiO_2@NH_2$  was formed in acetonitrile as a solvent solution, using ethylene glycol dimethacrylate as the cross-linker, building monomer, 1,1'-Azobis(cyclohexanecarbonitrile) as the radical initiator, methacrylic acid as a functional monomer and 4,4'-Dihydroxydiphenyl ether as the dummy template molecule as a structural analogue of low-mass PBDEs. To characterize the chemical structure of prepared DMMIPs, the Fourier transform infrared spectroscopy analysis was performed. The specific surface area of the developed sorbent was estimated using Brauner-Emmet-Teller nitrogen adsorption/desorption analysis. To assess the average pore sizes, pore diameters and pore volumes of the prepared sorbent, the Barret-Joyner-Halenda technique was applied. The average values of imprinting factor for PBDE-47 and PBDE-99 were  $11.3 \pm 1.6$  and  $13.7 \pm 1.2$ , respectively. The average value of recovery of PBDE-47 and PBDE-99 for developed DMMIPs from modelling water: methanol solution were  $85.4 \pm 6.7\%$  and  $86.4 \pm 9.4\%$ , respectively. In a case of spiked distilled water, tap water as well as local river water the calculated recovery values ranged from 65% up to 82% and from 33% up to 76% for PBDE-47 and PBDE-99, respectively. Following the preliminary research on selected water samples, the proposed combination of imprinting technology

\* Corresponding author at: Department of Analytical Chemistry, Faculty of Chemistry, Gdansk University of Technology, Gdansk, Poland, ul. Narutowicza 11/12, 80-233 Gdansk, Poland.  
 E-mail address: [marmarc@pg.edu.pl](mailto:marmarc@pg.edu.pl) (M. Marć).

and core-shell materials with magnetic properties might be considered as a promising sorption tool used for targeted recognition of low-mass PBDEs in aquatic solutions.

© 2020 The Authors. Published by Elsevier B.V. This is an open access article under the CC BY license (<http://creativecommons.org/licenses/by/4.0/>).

## 1. Introduction

Materials defined as the molecularly imprinted polymers (MIPs) are very specific types of analytical tools that constantly gaining the popularity in everyday laboratory practice. They are considered as a prevailing, smart generation of sorbent synthetic materials capable to precisely adsorb/bind a target chemical compound or a group of specific chemical compounds in preference to other similar chemicals in environmental, biological or food samples. The high scientific attention of MIPs is particularly caused by their wide spectrum of advantages mainly associated with high thermal, chemical and physical stability, relatively easy preparation process, reusability and cost-efficient mass preparation (Alves et al., 2019; Dinc et al., 2019). However, the most important aspect that new type of MIPs are constantly synthesised, characterised and introduced to analytical procedures is the fact that they significantly increase the accuracy, sensitivity and efficiency of the instrumental detection system as well as the sample preparation process (isolation and/or preconcentration process) (Speltini et al., 2017). Another advantage associated with MIP materials is the fact that they might be synthesised under laboratory conditions employing several polymerisation techniques, such as: bulk polymerisation, in-situ polymerisation, suspension polymerisation, dispersion polymerisation, dry phase inversion, precipitation, wet phase inversion, emulsion polymerisation, multi-steps swelling polymerisation (Ansari and Karimi, 2017). Depending on a performed type of polymerisation and its efficiency, it is possible to obtain MIP materials characterised by a different physico-chemical and morphological properties of MIPs particles. The optimal solution is to achieve imprinted materials characterised by spherical particles, optimal contact surface with the target molecules, as well as developed surface area and heterogeneous distribution of binding sites (Vasapollo et al., 2011; Cheong et al., 2013).

Generally, the selection of preparation process defines the potential application field of synthesised MIP material. Due to the several potential solutions in the field of MIPs preparation process, imprinted materials find the application as a key element and alternative solutions for commercially available materials in: (i) separation techniques - liquid chromatography (LC), capillary electrophoresis (CE), capillary electrochromatography (CEC), enantiomeric separations; (ii) sample preparation techniques - solid-phase extraction (SPE), solid-phase microextraction (SPME), dispersive solid-phase microextraction (DSPME) and their modifications; (iii) sensors and catalysis (Moein et al., 2019; Marć et al., 2018a; Ge et al., 2013).

The molecularly imprinted technologies (MIT) give a possibility to develop very specific sorption/binding materials, designed for an untypical chemical compound(s) or a new type of chemical compound(s) that were classified as a harmful or hazardous for the environment. It is a very promising solution, especially in a case when there is a lack of commercially available sorption materials (that might be applied in routine analytical procedures) or the recently available sorbents are characterised by insufficient selectivity, accuracy, efficiency and recovery. In addition, MIPs implementation in analytical procedure is a very good solution considering a chemical compounds that are present in environmental, biological or food samples at low or very low concentration level - the opportunity to carry out the isolation and/or preconcentration of analytes from samples characterised by complex matrix composition (Ansari and Karimi, 2017; Alexander et al., 2006; Ansari, 2017).

Nowadays, the molecules imprinted technology that successfully gaining in popularity are magnetic MIPs (MMIPs or mag-MIPs) - magnetic nanoparticles that are characterised by high dispersion stability

and good functional modification. In the Fig. 1 the information gathered from Scopus data base about the number of research articles in which application of various types of magnetic MIPs was described. Following this data it might be observed that during the last two decades there is a constant growth in a number of preparations and application of new types of magnetic MIPs in separation and extraction process (Xu et al., 2012).

Magnetic MIPs might be prepared in laboratory conditions based on iron, cobalt, nickel and their oxidizing material or alloy and are characterised by very good magnetism and specifically recognize abilities. Among these substrates, magnetic nanoparticles/nanospheres made of low toxicity iron oxide (core-shell  $\text{Fe}_3\text{O}_4$ @MIP) are the most often employed as a core/support to the layer of the imprinted polymer (He et al., 2014; Kubo and Otsuka, 2016). Another positive aspect of magnetic core-shell MIPs is the fact, that they might be separated from the solution attaching external magnet, without a need of centrifugation or filtration (costs and time reduction). That's why implementation of magnetic MIPs in analytical procedures might be considered as a "green" solution, following the philosophy of green analytical chemistry. The application of magnetic MIPs during the sample preparation process is not very complicated (Niu et al., 2016). Additionally, their use is very time-saving, gives a possibility to use small amounts of the sample and solvents, as well as the small volume of wastes are generated. Presently, magnetic core-shell molecularly imprinted materials is one of the most frequently employed sample separation and preparation approaches for the isolation and/or enrichment of specific type of analytes or group of chemical compounds in the field of liquid or semi-liquid food, environmental, as well as biological samples (Roció-Bautista et al., 2017; Speltini et al., 2017; Zhang et al., 2013; Gai et al., 2010; Hu et al., 2011).

A very specific type of analytes, classified as semi-volatile organic compounds (SVOC) that might occur in aquatic mediums such as river, sea or lake water, at low or very low content level are polybrominated diphenyl ethers (PBDEs). The PBDEs (mainly penta- and octa-BDEs) are considered as a relatively new environmental xenobiotics, because of the fact that they were attached on the list of Persistent Organic Pollutants (POPs) by the Stockholm Convention Committee in 2009 (Stockholm Convention, 2010). The PBDEs are one of the main group of flame retardants (FR) that were (or still are) employed as additives to polymeric materials, textiles, foams or building and indoor equipment elements. Their application process in a polymeric material is based on their dissolution, not covalent bond/attachment to the structure of the final material. Because of this, PBDEs might be leached out, migrate or be transported by the air masses to the various elements of the surrounded environment (Gustavsson et al., 2017). Moreover, because of their high stability in the environment and lipophilic character, they might occur in the wide spectrum of environmental elements for a very-long time period, as well as might be accumulated in tissues of living organisms (de Wit et al., 2010). However, about the PBDEs, the biggest concern in terms of the environmental impacts associated with their use, is their negative impact on living organisms. It is caused by their high neurotoxic potential, negative impact on a liver, as well as they might disturbing thyroid hormone homeostasis. Especially, they have very hazardous influence on the aquatic biota and whole aquatic food chain. Looking forward, the PBDEs might be absorb (accumulate) in a fish tissue and then by their consumption be directly transported to the human organism (Wang et al., 2015; Choo et al., 2018; Watanabe and Sakai, 2003). Despite the fact, that PBDE compounds enclose 209 congeners, the most frequently analytical procedures are developed and apply for determination of



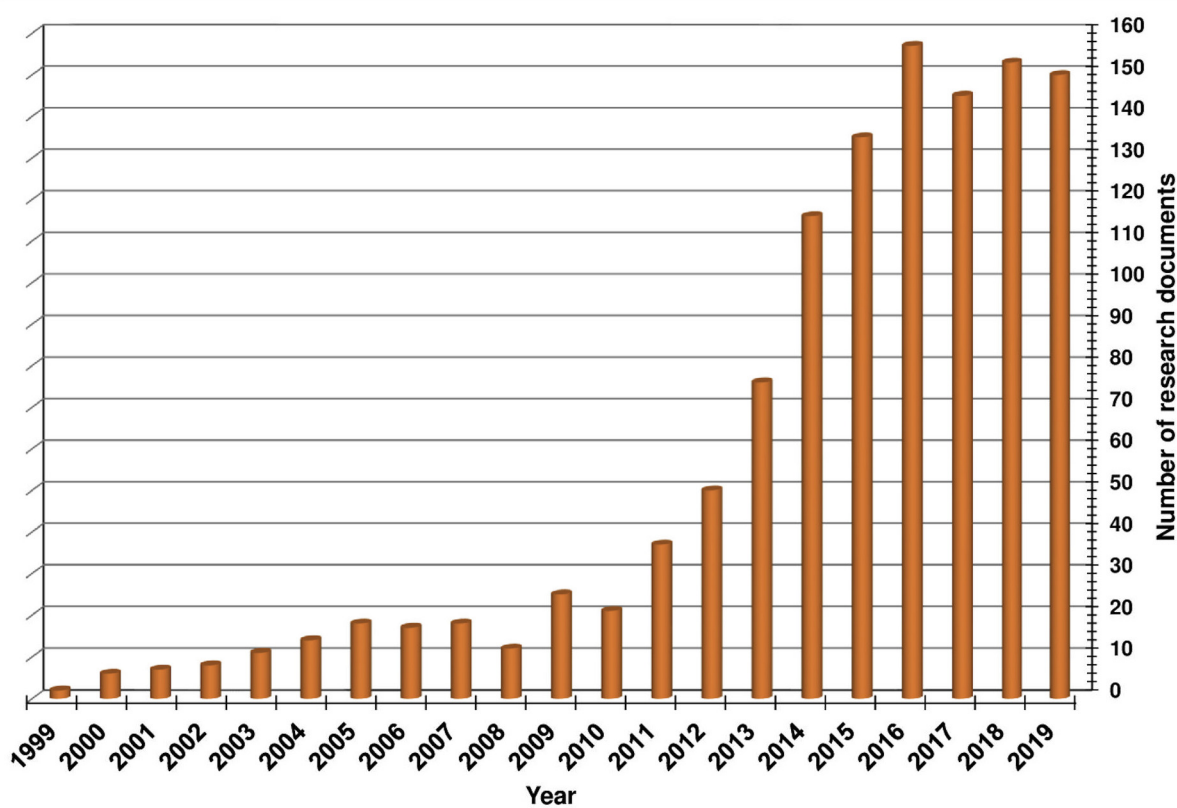


**Fig. 1.** The number of research documents published over the last two decades that concerns the application of new type of magnetic MIPs materials in the field of analytical chemistry [Scopus web site data base].

congeners classified as penta-BDEs: PBDE-47, PBDE-99, PBDE-100, PBDE-153, and PBDE-154. Regardless of the European Union (EU) decision in 2004, to ban the use of pentaBDEs as well as octaBDE, they are still present in various elements of the environment (Stapleton, 2006). It is mainly caused by their persistence potential and they might be produced by the debromination process of BDE-209 (Yan et al., 2018). Nowadays, the main research area in a case of penta-BDEs is focused on their determination in the mangrove, mudflat, open sea, freshwater pond, and bottom sediment which are typical parts of ecosystems in aquatic environments (Pan et al., 2018). PBDE-47 and PBDE-99 are characterised by the best water solubility (at 25 °C) –  $2.5 \cdot 10^{-4}$  and  $6.2 \cdot 10^{-5} \text{ g} \cdot \text{L}^{-1}$ , respectively (Komolafe et al., 2019) from all of penta-BDEs, that's why they are the most frequently monitor in a wide spectrum of aquatic media, mainly local rivers and lakes (Yan et al., 2018). Nevertheless, the main issue in determination process of penta-BDEs is the fact that they might occur in the aquatic environment at very low concentration levels. This is the main reason that analytical protocols dedicated for the analysis of PBDEs should be constantly improved, especially in the field of sample preparation process. There are a number of isolation and/or preconcentration techniques employed for PBDEs determination which were described in detail in several review papers. Most of them are characterised by multistep procedure, high costs of equipment exploitation, long time of single analysis and is some solutions the use of significant amount of organic solvents (Król et al., 2012; Berton et al., 2016; Pietroń and Małagocki, 2017). Because of this, still there is a need to develop and introduce to laboratory practice a new type of solutions that reduce the time of sample preparation process as well as reduce the organic solvents consumption.

The main aim of the research was to synthesise and study the binding abilities, particles morphological properties and potential field of application of magnetic MIP for preliminary recognition of the selected low-mass polybrominated diphenyl ethers, classified as a penta-BDEs

(PBDE-47 and PBDE-99) from selected spiked aqueous solutions. The studies were performed using surface modification technique, with the use of iron oxide ( $\text{Fe}_3\text{O}_4$ ) nanopowder as the main magnetic core. Furthermore, structural analogue of low-mass PBDEs was used as a dummy-template molecule - 4,4'-Dihydroxydiphenyl Ether. In addition, during the performed research several problems and challenges in the described dummy-template magnetic MIP preparation process have been encountered and were briefly discussed in this paper.

## 2. Materials and methods

### 2.1. Chemicals and reagents

Firstly, methacrylic acid (Merck KGaA, Darmstadt, Germany) - MAA (containing 250 ppm of MEHQ as inhibitor, 99%) and ethylene glycol dimethacrylate - EGDMA (Merck KGaA, Darmstadt, Germany) (98%, containing 90–110 ppm of monomethyl ether hydroquinone as inhibitor) were subjected to purification to remove the polymerisation inhibitors. The 1,1'-azobis (cyclohexanecarbonitrile) - ACHN (98%) and acetonitrile - ACN (isocratic grade for liquid chromatography LiChrosolv®), methanol (for liquid chromatography LiChrosolv®), tetraethylorthosilicate - TEOS (reagent grade, 98%), (3-aminopropyl) triethoxysilane - APTES (99%), toluene (anhydrous, 99.8%) and  $\text{Fe}_3\text{O}_4$  nanopowder (50–100 nm particle size, 97% trace metals basis) were purchased from Merck KGaA, Darmstadt, Germany. The ammonia solution ( $\text{NH}_3 \cdot \text{H}_2\text{O}$ , 25%) and isopropanol (analytical grade) were obtained from POCH, Gliwice, Poland). The 2,2,4-trimethylpentane (>99%) was delivered by ThermoFisher, GmbH, Germany. The 4,4'-Dihydroxydiphenyl Ether (4,4'-Oxydiphenol, >98%) used as a structural analogue for low mass PBDEs was supplied by TCI, Japan. The certificate reference standard solutions of selected low-mass PBDEs - the PBDE-47 (2,2',4,4'-Tetrabromodiphenyl ether,  $50 \mu\text{g} \cdot \text{mL}^{-1}$  in isooctane) and

PBDE-99 (2,2',4,4',5-Pentabromodiphenyl ether,  $50 \mu\text{g}\cdot\text{mL}^{-1}$  in isooctane) were delivered from LGC Standards (Teddington, United Kingdom).

All chemicals used in the study were of analytical grade and were utilized in the experiments in their original form without any further processing.

## 2.2. Apparatus

As for the glass laboratory equipment, the round-bottom flask (250 mL), round-bottom Schlenk flask (50 mL), glass plugs, Pasteur pipettes, glass thermometers up to  $200^\circ\text{C}$ , glass pipettes, Petri dishes, screwed glass flasks (22 mL), chromatographic amber screw vials (1.8 mL) and glass desiccator were employed. As a source of ultrasounds the stationary ultrasonic bath with frequency output 42,000 Hz (Cole-Parmer Instrument Company) was applied. The analytical equipment used at the stage of final determination stage was as follows: gas chromatograph (Agilent Technologies 7890A GC System) combined with mass spectrometer (Agilent Technologies 5977A MSD) system working in a selective ion monitoring mode - SIM mode (monitored ions  $m/z$  for PBDE-47: 324; 326; 484; 486; and PBDE-99: 404; 406; 564; 566) with quadrupole mass analyser. The GC-MSD was connected with Agilent 7693 autosampler. Mentioned GC-MSD system was also equipped with the pulsed splitless injector which initial temperature was set to  $300^\circ\text{C}$ , the injection pulse pressure was 25 psi until 1.5 min. The Agilent J&W HP-5,  $30 \text{ m} \times 0.25 \text{ mm} \times 0.25 \mu\text{m}$  fused silica capillary chromatographic column was used for the analysis of selected low mass PBDE compounds. The GC oven working programme was set as follows: initial temperature -  $90^\circ\text{C}$  held for 1 min, next increased at a rate of  $20^\circ\text{C}\cdot\text{min}^{-1}$  up to  $295^\circ\text{C}$ , and held for 10 min. The inert GC gas flow (He, 5.0) rate was set in the constant flow mode -  $1.2 \text{ mL}\cdot\text{min}^{-1}$ . The MSD ion source temperature was adjusted to  $250^\circ\text{C}$ , the MSD quad temperature was adjusted to  $150^\circ\text{C}$ . The transfer line between GC and MSD temperature was adjusted to  $300^\circ\text{C}$ . Each time  $1 \mu\text{L}$  of the analysed sample (analytical standard, calibration curve solution or real sample solution) was injected by the autosampler in splitless mode. The more information and detailed description of chromatographic analysis of PBDEs compounds might be found in previous literature data (Marć et al., 2018b; Król et al., 2014; Pountney et al., 2015).

The specific surface areas of the prepared DMMIP, as well as parallel MNIP were assessed using Brauner-Emmet-Teller (BET) nitrogen adsorption/desorption analysis. To evaluate the pore volumes, pore diameters as well as average pore sizes of the obtained DMMIP material and its equivalent MNIP, the Barret-Joyner-Halenda (BJH) technique was employed. Mentioned analysis were carried out employing Accelerated Surface Area and Porosimetry Analyzer (Micromeritics, model ASAP, 2020).

In order to receive the preliminary information about the characteristics of the chemical structure of the synthesised surface modified sorption materials (DMMIP and equivalent MNIP) the Fourier transform infrared spectroscopy (FT-IR) analysis was implemented. The FT-IR analysis of the prepared imprinted and non-imprinted materials and the efficiency of template washing process were recorded with a Nicolet Spectrometer IR200 from Thermo Scientific (Waltham, MA, USA). The device was equipped with an ATR attachment with a diamond crystal. Measurements were carried out with  $1 \text{ cm}^{-1}$  resolution in the range from  $4000$  to  $400 \text{ cm}^{-1}$  and 64 scans. The thermal analysis of developed DMMIP, MNIP and basic  $\text{Fe}_3\text{O}_4$  was performed using model TG 209F3 from NETZSCH (Germany). Samples of sorption materials weighing approx.  $7.0 \text{ mg}$  were placed in a corundum dish. The study was conducted in an inert gas atmosphere - nitrogen (flow rate  $20 \text{ mL}\cdot\text{min}^{-1}$ ) in the range from  $35$  to  $900^\circ\text{C}$  with a temperature increase rate of  $10^\circ\text{C}\cdot\text{min}^{-1}$ .

Scanning electron microscopy (SEM) images of prepared DMMIP and basic  $\text{Fe}_3\text{O}_4$  were taken with S-3400 N microscope (Hitachi,

Japan) in secondary electron mode. The accelerating voltage applied was  $15 \text{ kV}$ . No further pre-treatment was taken.

## 2.3. Synthesis of low-mass PBDEs dummy-template magnetic molecularly imprinted polymer particles

### 2.3.1. Preparation of $\text{Fe}_3\text{O}_4@\text{SiO}_2$ nanoparticles

To perform the modification of the surface of  $\text{Fe}_3\text{O}_4$  nanopowder by silica group ( $\text{SiO}_2$ ), approx.  $1 \text{ g}$  ( $0.9831 \text{ g}$ ) of  $\text{Fe}_3\text{O}_4$  nanopowder was dispersed into mixture of  $50 \text{ mL}$  of isopropanol and  $10 \text{ mL}$  of ultra-pure water in a round-bottom glass flask and then sonicated in ultrasonic bath for  $20 \text{ min}$  at room temperature. After this,  $10 \text{ mL}$  of ammonium hydroxide ( $\text{NH}_3\cdot\text{H}_2\text{O}$ ,  $25\% \text{ v/v}$ ) and  $5 \text{ mL}$  of TEOS were added dropwise. Next, the glass flask was placed in the ultrasonic bath for  $40 \text{ min}$  at room temperature. Then, the mixture was reacted for  $12 \text{ h}$  at room temperature under continuous vertical stirring. Finally, the resultant blackish grey product was separated attaching the external magnet. Obtained  $\text{Fe}_3\text{O}_4@\text{SiO}_2$  were washed three-times with distilled water and isopropanol and then dried under nitrogen gas atmosphere at  $60^\circ\text{C}$  for approx.  $1 \text{ h}$ . Prepared magnetic nanoparticles were transferred on a Petri dish and placed in glass desiccators.

### 2.3.2. Preparation of $\text{Fe}_3\text{O}_4@\text{SiO}_2@\text{NH}_2$

Approx.  $400 \text{ mg}$  of freshly prepared  $\text{Fe}_3\text{O}_4@\text{SiO}_2$  nanoparticles were dispersed in  $30 \text{ mL}$  of anhydrous toluene and functionalized by  $1 \text{ mL}$  of APTES in round-bottom Schlenk flask ( $50 \text{ mL}$ ). Mentioned flask with mixture was placed in ultrasound bath for  $10 \text{ min}$  at room temperature, next purged with nitrogen and then the solution was reacted for  $24 \text{ h}$  with the continuous vertical stirring. Finally, the flask was once again sonicated for  $10 \text{ min}$ , the magnetic particles were collected by the attached external magnet and washed several times by isopropanol and then dried under nitrogen gas atmosphere at  $50^\circ\text{C}$  for  $12 \text{ h}$  for further use.

### 2.3.3. Synthesis of DMMIP and MNIP

The preparation process of DMMIP was performed according to the following procedure. In a round-bottom Schlenk flask ( $50 \text{ mL}$ ) approx.  $100 \text{ mg}$  of freshly prepared  $\text{Fe}_3\text{O}_4@\text{SiO}_2@\text{NH}_2$  was dispersed in  $12 \text{ mL}$  of acetonitrile (ACN) and  $61.5 \pm 0.5 \text{ mg}$  of 4,4'-dihydroxydiphenyl ether (approx.  $0.3 \text{ mmol}$ ) as a dummy template for low-mass PBDEs. Next, the mixture was sonicated in the ultrasonic bath for  $20 \text{ min}$ . Then,  $130 \mu\text{L}$  of MAA (approx.  $1.2 \text{ mmol}$ ) was added, and the glass flask with reaction mixture was sonicated for  $10 \text{ min}$ . Next, the potential oxygen was removed under the nitrogen stream atmosphere, and the flask was plugged tightly, placed in dark and the solution was self-assembly for  $12 \text{ h}$  at room temperature to create template-monomer complex. After this, the very small magnetic stirrer was placed inside the flask and  $1.15 \text{ mL}$  of EDGMA (approx.  $20 \text{ mmol}$ ) was added as a cross-linker and then the glass flask was placed in a thermostatic oil bath and nitrogen gas supply tube was connected. Next, approx.  $100 \text{ mg}$  of reaction initiator ACHN was added, and the mixing device was set to the maximum rate to maintain the vigorous stirring. Finally, the polymerisation mixture was flushed by nitrogen stream for  $15 \text{ min}$  to remove the potential oxygen residues, the glass flask was tightly sealed and the polymerisation was performed at  $82 \pm 2^\circ\text{C}$  of oil bath (mixture temperature  $>80^\circ\text{C}$  causes rapid decomposition of applied free radicals initiator) for  $24 \text{ h}$ . After the polymerisation process, prepared DMMIP nanoparticles were collected by the attached external magnet and washed several times with methanol to totally remove the dummy template from the imprinted polymer structure and to remove potential reagents remaining from the preparation process. At the end DMMIP nanoparticles were dried first under the nitrogen stream atmosphere and then transfer to the Petri dish and dried at  $60^\circ\text{C}$  for  $12 \text{ h}$ . The effectiveness of the washing process was checked performing the FT-IR analysis. After drying process, Petri dishes with DMMIP were out inside the glass desiccators. The equivalent non-imprinted magnetic

nanoparticles (MNIP) were prepared following the same procedure in the absence of dummy template molecules during synthesis.

#### 2.4. Binding experiment and imprinting efficiency studies

Following the literature data associated with the calculation of sorption capacity/binding abilities, values of adsorption capacity ( $Q_t$ ) [ $\text{ng} \cdot \text{mg}^{-1}$ ] at the sorption equilibrium, in both static and dynamic binding experiments, were calculated based on the following Eq. (1) (Hashemi et al., 2017; Gao et al., 2018):

$$Q_t = \frac{C_0 - C_t \times V}{m} \quad (1)$$

The Eq. (1) variables defined as  $C_0$  and  $C_t$  represents the initial and final concentration of the appropriate low mass PBDE in prepared solution [ $\mu\text{g} \cdot \text{mL}^{-1}$ ]. As for the  $V$  and  $m$  equation's variables there are associated with sample volume [mL] and the weight of introduced DMMIP or its parallel MNIP [mg], respectively.

In general, the sorption capacity of prepared DMMIP and its adequate MNIP (blank sample) was calculated considering the difference of appropriate low mass PBDEs content level in the initial solution (defined content level of appropriate low mass PBDE compound), and their content level measured in supernatant collected above the DMMIP and its equivalent MNIP, after defined mixing time.

##### 2.4.1. Static binding abilities tests

To assess the binding/sorption capacity of prepared DMMIP as well as its equivalent NMIP, approx.  $32.6 \pm 1.7$  mg of DMMIP or approx.  $32.8 \pm 1.9$  mg of MNIP was introduced into 3 mL of methanol solution prepared in 10 mL glass flask. The prepared modelling solutions contain different content levels of defined low mass PBDEs, in the range from  $0.10 \mu\text{g} \cdot \text{mL}^{-1}$  to  $2.00 \mu\text{g} \cdot \text{mL}^{-1}$ . Next, the mixtures containing magnetic sorbent were shaken at 300 rpm for 8 h at room temperature to reach the appropriate sorption equilibrium. After that, the supernatant and the magnetic sorbents were separated by putting on an external magnet. The concentration of defined low mass PBDEs in the supernatant (volume reduced under nitrogen gas atmosphere to 1 mL) was measured by GC-MSD system, after filtered through  $0.22 \mu\text{m}$  membrane filter. Each sample was injected four times into GC-MSD system.

In order to assess the equilibrium parameters, as well as the capacity of adsorption of the selected low-mass PBDEs on prepared DMMIP and its parallel MNIP, the Freundlich (2) and Langmuir (3) linear isotherm models were employed. For this reason, the following general equations were applied (Khan et al., 2015; Khan et al., 2018; Seraj et al., 2020):

$$\ln(Q_e) = \ln(K_f) + \frac{1}{n} \ln(C_e) \quad (2)$$

$$\frac{C_e}{Q_e} = \frac{1}{K_L \times Q_m} + \frac{C_e}{Q_m} \quad (3)$$

The Eqs. (2), (3) variables defined as  $Q_m$  is the maximum sorption capacity [ $\text{ng} \cdot \text{mg}^{-1}$ ],  $K_L$  [ $\text{mL} \cdot \text{ng}^{-1}$ ] is associated with the Langmuir constant,  $K_f$  [ $\text{mL} \cdot \text{mg}^{-1}$ ] and  $n$  represents the constants of the Freundlich model. Following the literature data the  $n$  (or  $1/n$ ) is an empirical factor generally associated with to the sorption intensity, which is closely related to the material heterogeneity (Guo et al., 2019). As for the  $C_e$  and  $Q_e$ , they stands for equilibrium concentrations [ $\mu\text{g} \cdot \text{mL}^{-1}$ ] and equilibrium sorption capacity [ $\text{ng} \cdot \text{mg}^{-1}$ ], respectively.

##### 2.4.2. Dynamic binding abilities tests

In the dynamic binding abilities experiments were performed on approx.  $33.0 \pm 1.3$  mg of DMMIP or approx.  $32.4 \pm 2.0$  mg of its equivalent MNIP. Defined mass of magnetic sorbent was added into 3 mL of modelling methanol solution in a 10 mL glass flask. The modelling solution contains defined content levels of selected low mass PBDEs – 0.25

$\mu\text{g} \cdot \text{mL}^{-1}$ . The prepared samples were incubated at room temperature and shaken vigorously at 300 rpm for different time intervals: 15 min, 30 min, 45 min, 60 min, 90 min, 120 min, 180 min, 240 min, and 300 min. Next, the appropriate DMMIP or its analogous MNIP was separated by putting an external magnetic, the supernatant was collected, filtered through  $0.22 \mu\text{m}$  membrane filter and the mass of added low mass PBDEs in supernatant (previously the volume of the analysed sample was reduced to 1 mL) was measured by GC-MSD system. Each sample was injected four times into GC-MSD system.

In order to evaluate and graphically describe the adsorption mechanism of prepared DMMIP and its adequate MNIP towards selected low-mass PBDEs, pseudo-first-order (4) as well as pseudo-second-order (5) kinetic models were employed refers to the obtained experimental kinetic data. For this reason, the following general equations were used (Khan et al., 2015; Khan et al., 2018; Seraj et al., 2020):

$$\ln(Q_e - Q_t) = \ln(Q_e) - K_1 t \quad (4)$$

$$\frac{t}{Q_t} = \frac{1}{K_2(Q_e)^2} + \frac{t}{Q_e} \quad (5)$$

The Eqs. (4), (5) variables defined as  $K_1$  and  $K_2$  refers to pseudo-first order adsorption rate constant [ $\text{min}^{-1}$ ] and pseudo-second-order adsorption rate constant [ $\text{mg} \cdot \text{ng}^{-1} \cdot \text{min}^{-1}$ ], respectively. As for the  $t$ ,  $Q_e$  and  $Q_t$  they describes time of experiment [min], equilibrium sorption capacity [ $\text{ng} \cdot \text{mg}^{-1}$ ], and amount of adsorbate [ $\text{ng} \cdot \text{mg}^{-1}$ ] on adsorbent surface at time  $t$ , respectively.

#### 2.5. Determination of low-mass PBDEs in real samples – description of analytical protocol

During the potential application studies of developed DMMIP, three types of water samples were investigated – deionised water (pH – 4.4), tap water (pH – 6.8) and water collected from a nearby river (pH – 7.1). All samples were collected into a 0.5 L glass bottles, fully filled and storage at room temperature. Next, 3 mL of each sample was filtered with  $0.22 \mu\text{m}$  membrane filter to remove the insoluble impurities and placed into the 10 mL glass vials. Then, to each vial, the 0.30 mL of methanol was added to ensure the better solubility of standard solution of low-mass PBDEs (standard solutions are available in isooctane solution). After this, mentioned samples were spiked with the  $5 \mu\text{L}$  of low-mass PBDEs reference standard solution ( $c = 50 \mu\text{g} \cdot \text{mL}^{-1}$ ) and mixed for several minutes. Next, to the samples containing deionised water and tap water approx.  $33 \pm 2$  mg of DMMIP was added. As for the samples of river water, approx.  $43 \pm 2$  mg of prepared DMMIP was introduced. Next the prepared aquatic samples with magnetic sorbents were closed and shaking at 300 rpm for 6 h, at room temperature. After the shaking process, the external magnet was attached to separate the DMMIPs from the water solution. Next, the adsorbed low-mass PBDEs by developed DMMIP were extracted by adding 4 mL of isooctane solution and shaking at 300 rpm for 1 h, at room temperature. Then, the magnetic sorbent was separated from the isooctane solution by attaching the external magnet. Finally, the volume of eluent was reduced under the stream of nitrogen to 1 mL and the solution was transferred to the GC amber glass vials and analysed using GC-MSD system under previously described conditions. For each of the aquatic sample, six solutions with defined mass of DMMIP were prepared.

#### 2.6. Basic parameters of quality assurance/quality control

The calibration process was performed following protocol published in detail in previous papers (Marć et al., 2018b; Marć and Wiczeorek, 2019). In brief, the calibration process and the determination of calibration curves as well as the correlation coefficients (linearity) were carried out employing external standard method (ESTD). However, using the previously described GC-MSD system, it should be mention that

very often the sensitivity of mass spectrometer might undergo some clear changes during the analysis. For this reason, after the calibration process, during every series of measurements, the two closest content levels of calibration solutions to the analysed samples were selected to monitor the quality of the obtained results (restrictive solution method) and to perform the necessary corrections. Working standard solutions for calibration curves were prepared in isoctane: toluene (9:1 v/v), basing on a reference standard solutions of PBDE-47 and PBDE-99 at  $50 \mu\text{g} \cdot \text{mL}^{-1}$ . Six calibration solutions at ranged from 0.033 to  $2.0 \mu\text{g} \cdot \text{mL}^{-1}$  were employed to create the calibration curves for selected low-mass PBDEs as well as to establish the linearity ranges. Each of calibration solution was analysed nine times (nine replicate injections for all of content levels) and each time the volume of injected calibration solution was set to  $1 \mu\text{L}$ . The analysis of injected samples of calibration solutions was carried out using analytical equipment which working parameters and conditions were mentioned above as well as in previous papers (Marć et al., 2018b; Marć and Wiczorek, 2019). The calculated numerical values of  $R^2$  parameter (coefficient of determination) were as follows: for PBDE-47 the  $R^2 = 0.993$ , for PBDE-99 the  $R^2 = 0.991$ . The calculated values of standard deviation (SD) for each point on the created calibration curves were from 8.9 to 15.0%. SD value calculated for calibration solutions is mainly influenced by the ability to change the sensitivity of the applied mass spectrometer during the analysis of prepared samples.

To express the precision and repeatability of the performed research as well as the applied analytical procedure, the coefficient of variation (CV - as a percentage value of the ratio of the calculated standard deviation to the mean) was determined. In addition, based on the modelling solution research the recovery values, as well as the imprinting factor (IF) values were calculated for each of studied PBDEs. The precision and recovery of the applied analytical procedure and the determination of imprinting factor were investigated employing 5 mL of water: methanol (1:1 v/v) modelling solution containing defined concentration of each of selected low mass PBDEs ( $0.10 \mu\text{g} \cdot \text{mL}^{-1}$ ) in 10 mL glass flask with approx. 50 mg of DMMIP, as well as approx. 50 mg of its adequate MNIP. Next, the solution with magnetic sorbent was gently rotatory mixed by 1 h and after this the external magnet was attached to glass vial and modelling solution was discarded. Then, the back extraction was performed with the use of isoctane ( $2 \times 1 \text{ mL}$ ) each time attaching the external magnet to recover the magnetic sorbent. Next, the extract volume was reduced to 1 mL under a nitrogen stream atmosphere and transfer to the GC screw amber glass vial to perform the GC-MSD analysis. Six modelling solutions were prepared with a previously defined content level of low mass PBDEs and with appropriate mass of studied magnetic sorbent. For each of prepared modelling solution the GC-MSD analysis was repeated three times. The calculated CV values for PBDE-47 and PBDE-99 determined in modelling solutions were 14 and 12%, respectively. The calculated CV values do not exceed 20%, which might be considered as a sufficient result for future real samples analysis. As for the recovery parameter, the average value for PBDE-47 and PBDE-99 was  $85.4 \pm 6.7\%$  and  $86.4 \pm 9.4\%$ , respectively. The calculated values of recovery meets the requirements of the general assumptions, that in a case of low or very low concentration level of chemical compounds in environmental samples, the recovery values might range from 70% (even in some cases 50%) up to 120%. To assess the specific recognition capability of prepared DMMIP for selected low-mass PBDEs defined by the IF values, the following equation was employed (6) (Pupin et al., 2020; Khan et al., 2018):

$$IF = \frac{Q_{EDMIP}}{Q_{ENIP}} \quad (6)$$

The Eq. (2) variables defined as  $Q_{EDMIP}$  and  $Q_{ENIP}$  are associated with the binding capability of developed DMMIP on the selected low mass PBDEs and the binding capability of parallel non-imprinted magnetic material (MNIP) on the selected low mass PBDEs, respectively.

The values of the limit of detection (LOD) as well as the values of the limit of quantitation (LOQ) of the determined low-mass PBDEs were determined employing the signal-to-noise ratio of three and ten, respectively. The LOD values were calculated based on the injection of the calibration solution standard characterised by the lowest concentration level. The assessed values of LOD parameter were considered to approve their accuracy, verifying the following relation: (1)  $10 \times \text{LOD} > (\text{min mean value [ng]})$  and (2)  $\text{LOD} < (\text{min mean value [ng]})$ . The calculated values of LOD parameters fulfilled the mentioned requirements. The assessed values of the LOD for applied GC-MSD system were as follows: for PBDE-47 – 0.0102 ng; for PBDE-99 – 0.0105 ng.

Detailed information about the calibration process of the GC-MSD system and calculated basic validation parameters for the employed GC-MSD system was presented in previous papers (Marć et al., 2018b; Marć and Wiczorek, 2019).

### 3. Results and discussions

#### 3.1. The DMMIP particles surface structure and morphological characteristic

The information about the results of BET and BJH analysis considering the distribution of particles pore volume and pore surface area in comparison to particles pore diameter of prepared DMMIP and its corresponding MNIP was presented in the Fig. 2. Following the data presented in the Fig. 2 it might be observed a slight but clear difference between pore distribution profile of developed DMMIP and its corresponding non-imprinted magnetic material (MNIP). The overall morphological parameters of particles of developed magnetic sorbent and its equivalent non-imprinted material were as follows: (i) average pore surface area: DMMIP –  $15.99 \text{ m}^2 \cdot \text{g}^{-1}$ , MNIP –  $9.62 \text{ m}^2 \cdot \text{g}^{-1}$ ; (ii)

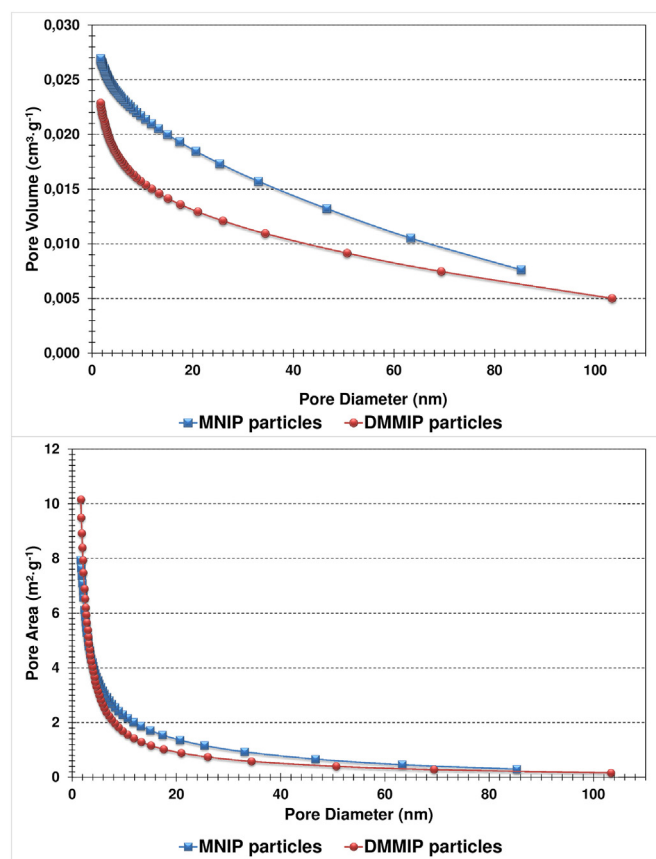


Fig. 2. The relationship between particles pore diameter, pore area and pore volume of prepared DMMIP and its equivalent MNIP material.

desorption average pore diameter: DMMIP – 9.01 nm, MNIP – 13.57 nm; (iii) desorption cumulative pore volume: DMMIP –  $0.021 \text{ cm}^3 \cdot \text{g}^{-1}$ , MNIP –  $0.027 \text{ cm}^3 \cdot \text{g}^{-1}$ ; the  $S_{\text{micro/t-plot}}$  parameter defining amount of mesopores: DMMIP –  $3.69 \text{ m}^2 \cdot \text{g}^{-1}$ , MNIP –  $0.84 \text{ m}^2 \cdot \text{g}^{-1}$ . Based on this data it might be concluded that  $\text{Fe}_3\text{O}_4$  particles covered by the thin film of the imprinted polymer were characterised more developed particles surface area, than its adequate MNIP (approx. 60% higher surface area of DMMIP than MNIP). Because of this prepared magnetic sorption material might be considered as a better sorbent in a case of low-mass PBDEs than its analogous non-imprinted material. In addition, prepared DMMIP is characterised higher amount of mesopores (above four times higher), that's why the availability of binding/sorption sites might be much better in comparison to MNIP – higher availability of DMMIP particles (mesopores) for the defined group of chemical compounds than equivalent MNIP. Furthermore, more developed particles surface area as well as the presence of higher amount of mesopores might be considered as another factor that proofs the presence of specific binding sites in polymer structure created on the magnetic nanoparticles surface. The high level of mesopores in the structure of polymeric material is a very desired phenomenon, because of the fact that they help to recognize and collect (bind) defined chemical compounds characterised by the similar chemical structure to the applied template (or dummy template). Finally, the presence of mesopores combined with the appropriate surface area and pore diameter gives a possibility to ensure the correct conditions of permeability (good migration of the aquatic sample through the polymer structure and increase the possibility to achieve the binding sites by selected chemical compounds) of the sample and organic solvents during the analyte collection as well as extraction process. The key element during the regular sorbents application or core-shell magnetic sorbents is to ensure the free migration of analytes towards binding sites and free solvent transport deep into the polymer structure, in order to reach specific binding sites.

The results of scanning electron microscopy (SEM) analysis were shown in Fig. 3. It was observed a clear difference between the morphological shape of basic  $\text{Fe}_3\text{O}_4$  nanoparticles and the morphological structure of synthesised DMMIP. It might be noticed that in some points the  $\text{Fe}_3\text{O}_4$  nanoparticles are covered by the thin-film of MIP material. In addition, prepared DMMIP particles are more dispersed than basic  $\text{Fe}_3\text{O}_4$  nanoparticles. It might result from the performed polymerisation process, as well as from the washing out of the template molecules from the structure of DMMIP. In addition it might be noticed that the surface of prepared DMMIP is less regular than basic  $\text{Fe}_3\text{O}_4$  and for this reason might characterised by higher surface area and by the presence of

specific binding cavities. According to Chang et al. (2012), Khan et al. (2018) and Zhang et al. (2018) attaching on the surface of  $\text{Fe}_3\text{O}_4$  the thin layer of the molecularly imprinted polymer gives a possibility of rapid kinetics and site accessibility – higher adsorption capability as well as improve the mass transfer rate.

To achieve the information about the surface characteristic of prepared DMMIP as well as the efficiency of the dummy-template washing/removing process the FT-IR analysis was performed. The results of FT-IR analysis for a basic  $\text{Fe}_3\text{O}_4$ , DMMIP and MNIP were shown in Fig. 4. According to the information shown on the Fig. 3 it might be observed a clear difference between basic  $\text{Fe}_3\text{O}_4$  and both DMMIP and MNIP. In addition, it might be observed a lack of characteristic IR peaks (mainly from O–H bonds in the range from 3450 up to  $3000 \text{ cm}^{-1}$  as well as the lack of characteristic strong peaks from C=C stretching vibration in the range from 1600 up to  $1580 \text{ cm}^{-1}$ ) from applied dummy-template (4,4'-Dihydroxydiphenyl ether) which is the proof that applied dummy template was successfully washed out from the imprinted polymer structure. Following the data presented on the Fig. 4 it might be noticed a high similarity of prepared DMMIP and its analogous MNIP. The presence of a weak peaks in the range  $2983\text{--}2939 \text{ cm}^{-1}$  might be associated with the appearance of antisymmetric and symmetric C–H stretching vibrations of the alkyl chains, and might be assigned to APTES (Xu et al., 2013). The presence of clear but weak peak at  $1632 \text{ cm}^{-1}$  might corresponds to the stretching vibration of N–H in APTES (Bayat et al., 2014; Gul et al., 2019). A presence of strong peak at  $1720\text{--}1710 \text{ cm}^{-1}$  generally is characterised for the C=O groups of applied cross-linker (EGDMA) grafted on the surface of magnetic core that confirmed the successful polymerisation process (Gao et al., 2018). The weak absorbance peak at  $\sim 750, 945$ , as well as approx.  $1052 \text{ cm}^{-1}$  might corresponds to the stretching vibration of the Si–O, Si–O–H, and Si–O–Si bonds, respectively. This might be the reason to believe that  $\text{SiO}_2$  layer was attached and covered the surface of the  $\text{Fe}_3\text{O}_4$  nanoparticles (Xie et al., 2015).

To estimate the thermal stability of developed magnetic sorption material, the thermal gravimetric analysis (TGA) was performed, and the results of this analysis (basic  $\text{Fe}_3\text{O}_4$ , DMMIP and MNIP) were shown in the Fig. 5. The curve of basic  $\text{Fe}_3\text{O}_4$  indicated the weight loss of 0.70%, and the main reason of this might be the evaporation of residual water. However, this leads to the conclusion that analysed basic  $\text{Fe}_3\text{O}_4$  nanoparticles were thermally stable in temperature ranges of  $35\text{--}900 \text{ }^\circ\text{C}$ . In a case of nanoparticles samples of DMMIP as well as corresponding MNIP the weight losses for them at around  $290 \text{ }^\circ\text{C}$  were 7.95% and 9.55%, respectively. The weight losses might be mainly associated with the evaporation of the physically adsorbed water or solvents

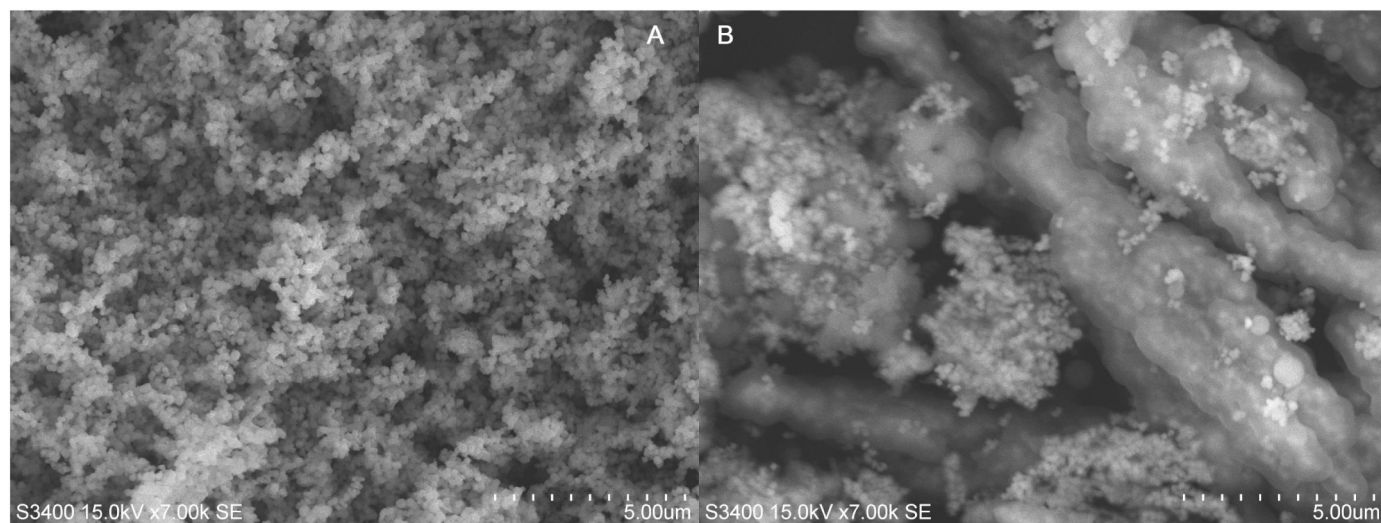


Fig. 3. The general view of surface morphology of basic  $\text{Fe}_3\text{O}_4$  (A) and prepared DMMIP (B) obtained by scanning electron microscopy studies.

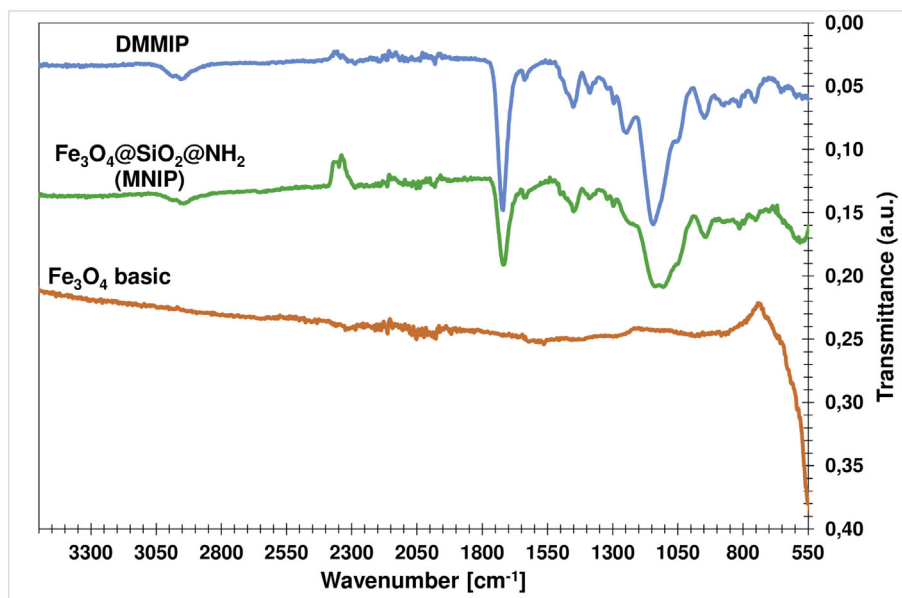


Fig. 4. The general view of FT-IR spectra of basic  $\text{Fe}_3\text{O}_4$ , prepared DMMIP and its corresponding non-imprinted core-shell magnetic polymer (MNIP).

residues. When the temperature changed gradually from 300 °C to 470 °C, the second mass losses were observed – 41.93% for DMMIP and 67.10% for MNIP. The weight loss of suggesting that structure of the imprinted polymer was successfully grafted on the surface of  $\text{Fe}_3\text{O}_4$  nanoparticles. The weight losses in this area mainly might be associated with the thermal degradation of the functional groups originate from the applied functional monomer (MAA) as well as the cross-linking agent (EGDMA). In addition, following the data shown on the Fig. 5 it might be concluded that DMMIP is characterised by good thermal stability and might be employed the further practical application. Moreover, the differences between DMMIP and MNIP thermal stability might be caused by the presence of specific wholes/binding site DMMIP surface structure, in grafting density during polymerisation process as well as the thermolysis of combustion products from previous stages.

### 3.2. The binding/sorption capabilities and imprinting efficiency studies

The results of performed research about the binding abilities – static and dynamic/kinetic sorption capabilities of developed DMMIP and its equivalent MNIP were shown in the Fig. 6. The error bars shown on the Fig. 6 are expressed by the SD values of obtained results (six repetitions for a single point). Considering the data shown in the Fig. 2 and described particle morphology characteristic in previous chapter it might be predicted that sorption abilities of prepared DMMIP will be better than in a case of its adequate MNIP. It might be associated with the higher surface area as well as the smaller pore volume and pore diameter of DMMIP. As for the kinetic sorption capabilities of studied magnetic materials for PBDE-47 and PBDE-99 presented in the Fig. 6a and b it might be observed a clear difference between magnetic material covered with the imprinted polymer and material covered with the non-

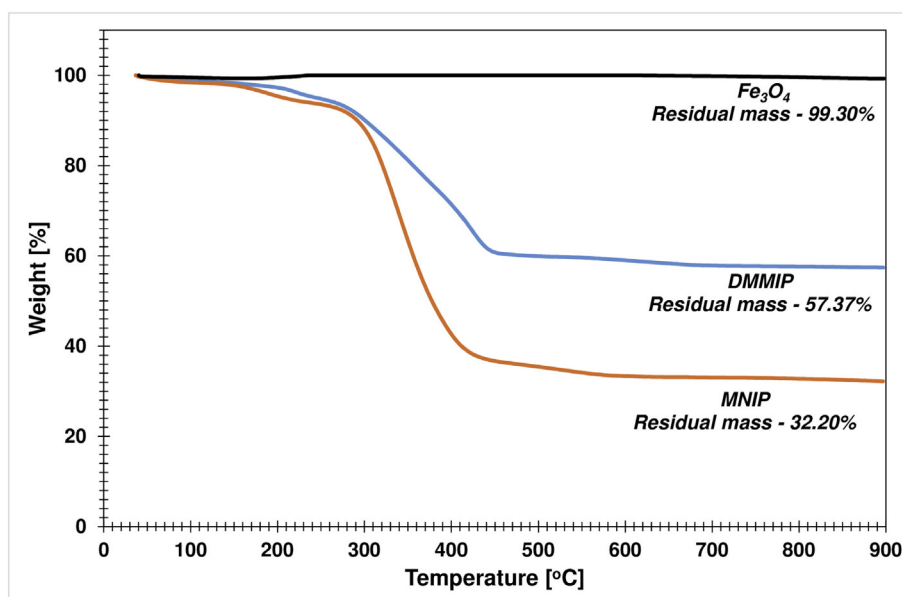


Fig. 5. The general view of TGA curves of basic  $\text{Fe}_3\text{O}_4$ , developed DMMIP as well as its parallel MNIP.



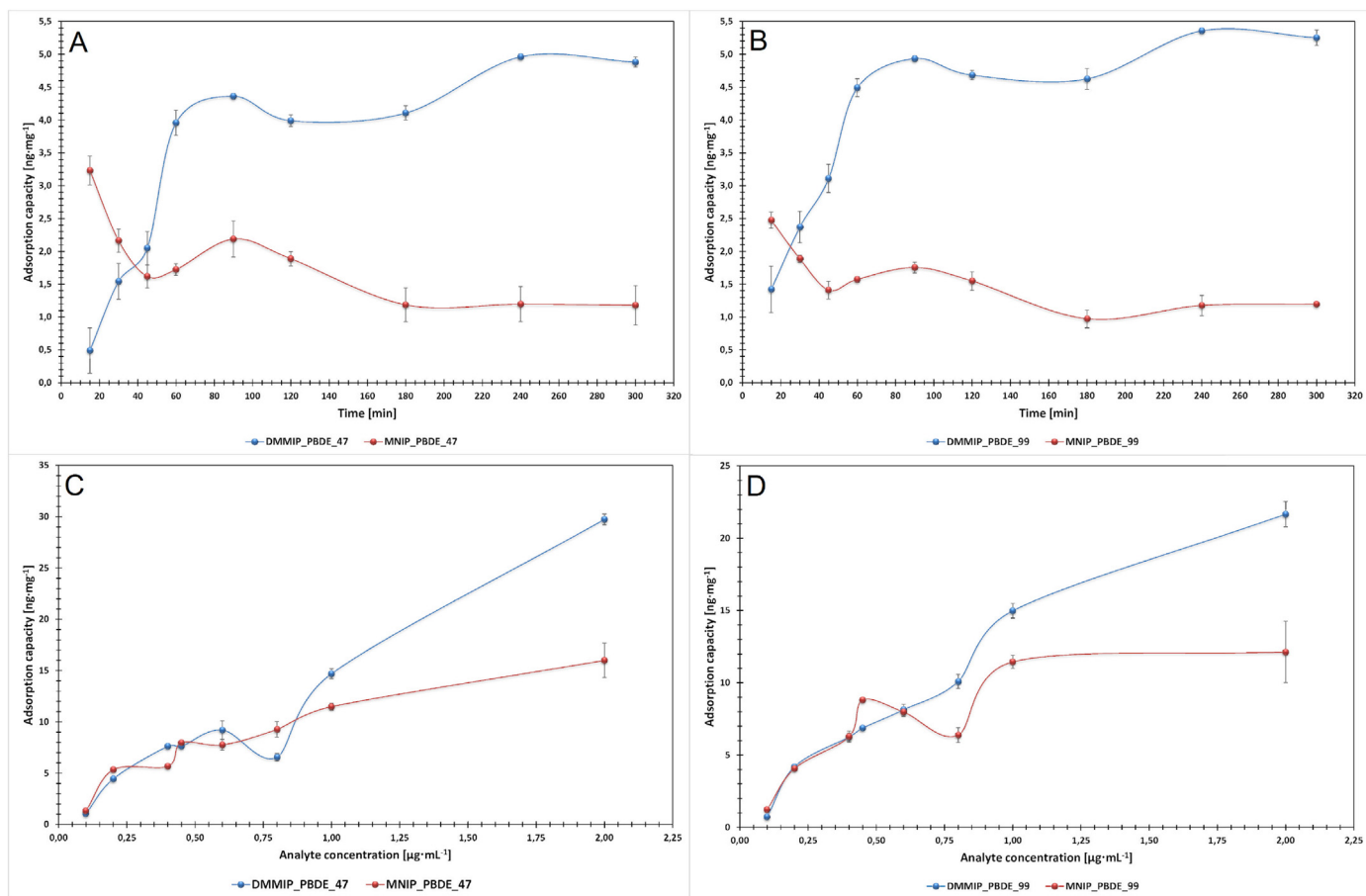


Fig. 6. The general view of binding affinity studies of prepared DMMIP and its analogue MNIP – static (A and B) and kinetic (C and D) adsorption characteristics.

imprinted polymer. A visual difference in sorption capability starts after 30 min from the initial point. The binding capacity of representatives of low-mass PBDEs on DMMIP gradually reaches equilibrium in the following 90 min with the maximum sorption capacity of  $4.88 \pm 0.10 \text{ ng} \cdot \text{mg}^{-1}$  and  $5.25 \pm 0.12 \text{ ng} \cdot \text{mg}^{-1}$  for PBDE-47 and PBDE-99, respectively. The presence of this phenomenon might be caused by the occurrence of specific binding sites on the surface of a layer of sorption material attached to the magnetic core. Moreover, the solubility of analysed compounds in aquatic solution (even in prepared modelling solution water: methanol) is very hard, because of this there is possibility that analysed compounds might be also adsorbed in standard physical (Van der Waals) adsorption process on the surface of applied sorption material. The presence of the special binding sites on the surface of prepared DMMIP as well as their availability, additionally increases the sorption abilities of employed magnetic sorption material. There is a possibility that, the thin imprinted polymer film could enable the rapid mass transport within the thin layer, which makes the specific binding sites more accessible for the studied analytes (Zhang et al., 2018). Interesting observation might be the fact, that in a case of DMMIP after 90 min from the initial point, after reaching almost equilibrium point, sorption material was characterised by slightly sorption fluctuations. Probably, it might be caused by the unavailability of all selective cavities (specific binding sites) in defined mixing time. As for the non-imprinted magnetic nanoparticles (MNIP) it might be noticed a reverse phenomenon. The maximum sorption abilities analysed MNIP reach before 30 min from the initial point. After 30 min, consequently (in several points with some slight fluctuations) the sorption abilities of MNIP decrease and reach the equilibrium point after 180 min. The maximum sorption capacity obtained by the MNIP was  $1.180 \pm 0.017 \text{ ng} \cdot \text{mg}^{-1}$  and  $1.20 \pm 0.30 \text{ ng} \cdot \text{mg}^{-1}$  for PBDE-47 and PBDE-99,

respectively. The presence of this phenomenon and characteristic of sorption abilities of MNIP might be explained by the lack of specific binding sites in the structure of polymer material attached to the magnetic core, as well as of its weakly developed particles surface. In addition, the decrease of the sorption abilities of non-imprinted magnetic material might be associated with the fact that analysed low-mass PBDEs are spontaneously collected on the surface of MNIP mainly by the conventional (standard) physicochemical adsorption. With high possibility it might be stated, that there is a lack of specific binding sites that will increase the binding abilities of studied material. The adsorption phenomenon that occurs in a case of non-imprinted magnetic materials placed in modelling solution might be the result of low solubility of studied low-mass PBDEs and their adsorption potential on the surface of solid materials. In comparison, the binding capacity of MNIP sorption material is much lower than that of prepared DMMIP in the whole period. Furthermore, there is an observed gentle difference in sorption abilities for PBDE-47 and PBDE-99 in a case of DMMIP. Mainly it might be caused by the differences in the chemical structure of the analysed compounds as well as their solubility in modelling solution. As for the MNIP it might be stated that there is no statistical difference between sorption abilities for selected low-mass PBDEs, probably caused by the lack of specific binding sites in the structure of polymer material.

Taking into account the data shown in the Fig. 6c and d considered the static binding capabilities it also might be observed a visual difference between synthesised DMMIP and its equivalent MNIP. When the concentration of analysed low-mass PBDEs was in the range from 0.10 to  $0.60 \mu\text{g} \cdot \text{mL}^{-1}$  the sorption capabilities of studied materials raised gradually and the difference in a sorption abilities between prepared DMMIP and its equivalent MNIP were statistically insignificant. Probably, the reason of this is the occurrence of standard physical (Van der

Walls) adsorption of analysed compounds on the surface of sorption material, regardless of the presence of specific binding sites. In addition, referring to the DMMIP sorption material, it is possible that low-mass PBDEs in mentioned concentration range cannot reach to the specific binding sites. The phenomenon of conventional (standard) physico-chemical adsorption of selected low-mass PBDEs on the surface of both materials may result from the fact that these compounds are very hard to dissolve in the modelling solution and have a high affinity for the solid phase than for the liquid medium. Furthermore, in general the binding capabilities of prepared MNIP material to PBDE-47 and PBDE-99 might be caused by the intermolecular interactions such as the van der Waals forces. When the concentration of selected low-mass PBDEs in modelling solution was above  $0.80 \mu\text{g}\cdot\text{mL}^{-1}$  it might be noticed a clear difference between imprinted and non-imprinted magnetic sorbents. For the prepared DMMIP the calculated value (six repetitions of a single point) of sorption capacity at the final concentration of low-mass PBDEs set to  $2.0 \mu\text{g}\cdot\text{mL}^{-1}$  was  $29.7 \pm 1.7 \text{ ng}\cdot\text{mg}^{-1}$  for PBDE 47 and  $21.66 \pm 0.88$  for PBDE-99  $\text{ng}\cdot\text{mg}^{-1}$ . As for the non-imprinted magnetic sorbent at the same concentration of low-mass PBDEs the calculated value (six repetitions of a single point) of sorption capacity was  $16.00 \pm 0.53 \text{ ng}\cdot\text{mg}^{-1}$  for PBDE-47 and  $12.2 \pm 2.1$  for PBDE-99  $\text{ng}\cdot\text{mg}^{-1}$ . Moreover, it might be observed that the MNIP reaches almost the equilibrium state approx. above  $1.2 \mu\text{g}\cdot\text{mL}^{-1}$  which may probably result from saturation of sorption bed, caused by the low pore surface area. Regarding the DMMIP sorbents, the clear equilibration state was not reached and the sorption bed was not saturated. The occurrence of a visual difference in static sorption capabilities above the concentration of low-mass PBDEs equal  $0.80 \mu\text{g}\cdot\text{mL}^{-1}$  between prepared DMMIP and its analogues MNIP might arise as a result of the presence and availability of specific binding sites in the structure of polymer material attached to the magnetic core, as well as their particles morphological properties. Because of this developed DMMIP is able to identify and selectively collect mentioned representatives of SVOCs that might occurs in the aquatic environment at low or very low concentration level. Prepared DMMIP based on a proposed dummy template molecule is characterised by good affinity to the low-mass PBDEs and might be considered as potential magnetic sorption material in microextraction techniques for specific recognition of representatives of PBDEs.

Following the correlations demonstrated in the Eqs. (2) and (3), obtained static sorption data were transformed into linear form of Freundlich (Supplementary Fig. 1) and Langmuir (Supplementary Fig. 2) curves – isotherm models. As for the binding kinetic data, following the correlations present in Eqs. (4) and (5), the Lagergren's pseudo-first-order (Supplementary Fig. 3), as well as pseudo-second-order (Supplementary Fig. 4) kinetic curves were determined. The most important parameters based on the determined sorption isotherms and kinetic curves were calculated and listed in the Table 1. At this point it should be mentioned, that the studied imprinted material was prepared based on structural analogue of target analytes (low-mass PBDEs), due to this there is a possibility that sorption abilities and kinetic parameters might be slightly difficult to describe. In brief, following the information listed in the Table 1 and considering the data present in Supplementary Figures from 1 to 4, it might be observed that in a case of DMMIP the correlation coefficient ( $R^2$ ) calculated based on Freundlich model was more suitable than calculated based on Langmuir model. The opposite situation was observed for non-imprinted magnetic materials. The calculated values of maximum sorption capacity ( $Q_m$ ) for DMMIP were  $94.37$  and  $50.54 \text{ ng}\cdot\text{mg}^{-1}$  for PBDE-47 and PBDE-99, respectively. As for non-imprinted magnetic materials the NIP calculated values of maximum sorption capacity were  $23.18$  and  $15.34 \text{ ng}\cdot\text{mg}^{-1}$  for PBDE-47 and PBDE-99, respectively. However, it should be highlighted that in a case of DMMIP the determined value of  $R^2$  was very low –  $0.064$  (greater non-linearity). Following the data listed in the Table 1 about the sorption isotherms and literature information, it might be concluded that the sorption process in non-imprinted magnetic materials was

generally accomplished in monolayer – the lack of lateral interactions (Araghi and Entezari, 2015; Pupin et al., 2020). According to Demirci et al. (2017) and Seraj et al. (2020) the adsorption process that occurs on the surface of non-imprinted magnetic material might be the confirmation of the presence of homogeneous binding sites, that might be energetically equivalent – the lack of specific imprinted cavities. For this reason, following the data listed in Table 1, the Langmuir isotherm model is more suitable for MNIP. In a case of the magnetic imprinted polymer that might possess on its surface a specific binding sites/cavities, and in a consequence non-homogeneous surface, the Freundlich isotherm model is more appropriate. Furthermore, it might be assumed that there is a possibility of physical sorption on the surface of MNIP. As for DMMIP, there might be chemical interactions resulting from the arrangement of functional groups of polymer during imprinting process, which gives a reason to assume that chemical sorption is predominant.

Analyzing sorption kinetic models listed in a Table 1 and Supplementary Figs. 3 and 4 it was noticed that the obtained experimental results were in-line with the pseudo-second-order model (higher values of the correlation coefficient). The presence of this phenomenon might be the reason to believe that adsorption process on the surface of developed magnetic materials has chemical nature. Additionally, calculated values of equilibrium sorption capacity (obtained for pseudo-second-order kinetic model) for prepared DMMIP were much greater than its parallel MNIP, for selected low-mass PBDEs. This is consistent with the earlier relationship observed for the results obtained during the experimental studies.

Another factor that gives the information about the binding abilities of prepared DMMIP and well as the potential application field is associated with the evaluation of imprinting factor (IF) and the recovery values of determined chemical compounds from the aquatic solution. The general information about the estimated values of imprinting factor as well as the recovery values for selected four samples of DMMIP and its equivalent MNIP introduced to the modelling solutions containing selected low-mass PBDEs at concentration level equal  $0.10 \mu\text{g}\cdot\text{mL}^{-1}$  was presented in Fig. 7. The error bars presented in Fig. 7 concerns the SD values of injection repetitions of each sample ( $n = 6$ ) prepared with the use of DMMIP and its analogous MNIP. Due to the fact, that developed imprinted polymer was synthesised based on dummy template molecule, not on the typical PBDE compound, the selectivity coefficient ( $\alpha$ ) was not estimated. The values of  $\alpha$  coefficient is only calculated and possess the reliable meaning, when in the course of the polymer synthesis the employed template molecule is a direct representative of defined chemical compound or group of chemical compounds.

Following the data shown in Fig. 7 it might be observed that calculated values of IF were ranged from  $9.7$  up to  $13.4$  for PBDE-47 and from  $12.1$  up to  $15.0$  for PBDE-99. In a case of PBDE-47, the high value of IF might be associated with the symmetrical and similar chemical structure to the applied dummy-template (four bromine atoms, two at each of the aromatic rings). Because of this the main factor that impact on the high value of IF and bounding abilities of DMMIP in a case of PBDE-47 is the fact of similarity in chemical structure and appropriate fit to binding cavities present in the structure of the imprinted polymer. A slightly higher values of IF calculated for PBDE-99 might be explained by the two aspects, the presence of five bromine atoms in its structure and the lower solubility in water solution than PBDE-47. For this reason the PBDE-99 might be selective combined by the imprinted polymer not only by the specific binding sites but additionally by the more affinity to standard physical (Van der Walls) adsorption on the surface of the film of the imprinted polymer. Nevertheless, in both cases the IF value was significantly above 1, therefore it might be state that prepared DMMIP is characterised by the inordinate affinity for selected low-mass PBDEs. Such high IF value might also result from the fact that studies were carried out in a model aquatic solution (water: methanol) in which both PBDEs are properly dissolved and DMMIP particles are appropriately dispersed. Because of this, the mass transfer is not significantly disturbed and the binding cavities are available for defined type

**Table 1**  
Sorption isotherm and sorption kinetic parameters.

Calculated parameter/Sample		DMMIP		MNIP	
		PBDE-47	PBDE-99	PBDE-47	PBDE-99
Freundlich model	$n$	1.030	0.954	1.336	1.407
	$K_f \left[ \frac{mL}{mg} \right]$	14.328	13.794	11.435	10.111
	$R^2$	0.892	0.910	0.879	0.814
Langmuir model	$Q_m \left[ \frac{ng}{mg} \right]$	94.369	50.542	23.184	15.341
	$K_L \left[ \frac{mL}{ng} \right]$	0.176	0.363	0.989	1.743
	$R^2$	0.0643	0.727	0.888	0.839
Pseudo-first-order kinetic	$K_1 \left[ \frac{1}{min} \right]$	0.0035	0.0059	<i>n. d.</i>	<i>n. d.</i>
	$Q_e \left[ \frac{ng}{mg} \right]$	5.114	3.231	<i>n. d.</i>	<i>n. d.</i>
	$R^2$	0.714	0.731	<i>n. d.</i>	<i>n. d.</i>
Pseudo-second-order kinetic	$K_2 \left[ \frac{mg}{ng \times min} \right]$	0.00455	0.00134	<i>Negative value</i>	<i>Negative value</i>
	$Q_e \left[ \frac{ng}{mg} \right]$	7.001	5.984	1.099	1.109
	$R^2$	0.831	0.985	0.971	0.980

negative value – the graphical illustration of sorption abilities was a curve decreasing to lower limit (illustrated on Fig. 6A and B for MNIP), for this reason the negative values (as well as the lack of pseudo-first-order kinetic characteristic) were obtained; n. d. – not determined.

of chemical compounds. However, considering the literature data, in a case of magnetic-MIPs the IF values i.e. pesticides (in some cases characterised by similar chemical structure to low-mass PBDEs) are also significantly above 1 – for triazole and non-triazole pesticides IF values ranged from 2.45 up to 2.57 (He et al., 2019); for triazophos from 2.460 to 4.059 (Wu et al., 2019); for organophosphorous pesticides 1.60 up to 2.72 (Wei et al., 2018) and for organophosphorous insecticides from 1.0 up to 9.2 (Zuo et al., 2015). The differences in IF values are mainly caused by the different matrix composition, different MIP preparation process and different separation conditions.

As for the recovery values, for prepared DMMIP were ranged from 81% up to 92% for PBDE-47 and from 76% up to 96% for PBDE-99. In a case of corresponding MNIP, the recovery values were ranged from 4.6% up to 7.6% for PBDE-47 and from 4.9% up to 8.9% for PBDE-99. The recovery values for synthesised DMMIP for selected low-mass

PBDEs were over ten times higher in comparison to recovery values calculated for its equivalent MNIP. It might be believed that much higher recovery values calculated for DMMIP are the additional proof for the presence of specific binding sites/cavities in the structure of thin film of polymeric material. It might be also considered as the proof of imprinting effect as well as the fact that selected low-mass PBDEs are not only adsorbed on the surface of magnetic sorption material but also reach the specific binding sites.

### 3.3. Application in real environmental water samples

Prepared DMMIP nanoparticles were employed to assess their the application potential as a magnetic sorption material for selective recognition and isolation and/or enrichment selected low-mass PBDEs in deionised water, tap water as well as local river water. As it was

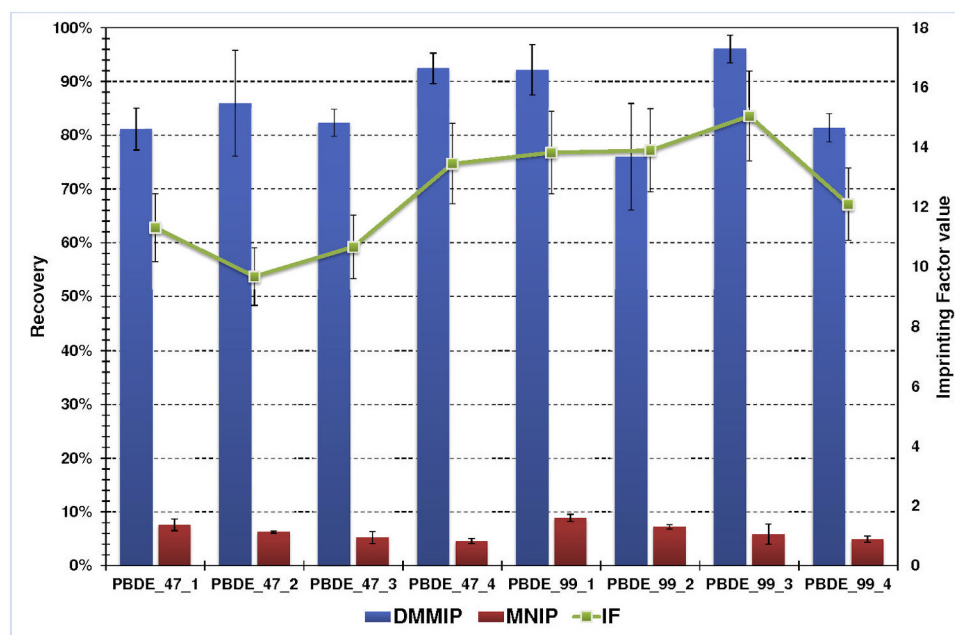


**Fig. 7.** The general calculated values of imprinting factor and recovery rates of analysed low-mass PBDEs measured in modelling solution (water: methanol, 1:1) with the use of prepared DMMIP and its corresponding MNIP.

previously mentioned, PBDEs compounds might occur in the aquatic medium at low or very low concentration level. For this reason, as it was described earlier, to assess the application potential of developed DMMIP, studied samples were spiked by defined amount of selected low-mass PBDEs (spiked with the 5 µL of low-mass PBDEs reference standard solution per studied water sample). The average values of calculated recovery rates for three types of studied spiked water samples were present in Fig. 8. The error bars are defined by the standard deviation values and ranged from 5.5% up to 17%. The range of recovery rates calculated for studied spiked samples were from 65% up to 82% and from 33% up to 76% for PBDE-47 and PBDE-99, respectively. The higher values of recovery calculated for PBDE-47 than for PBDE-99 might result from the similar (and symmetrical) chemical structure to the applied dummy template and the slightly better solubility in a water solution. Furthermore, the PBDE-47 might more easily reach specific binding sites/cavities and occupy them faster, thereby limiting PBDE-99 access. The recovery values for deionised water and river water as a representative of the aquatic environmental sample gives satisfactory results. In a case when the concentration of target analytes in environmental samples is at very low level, the acceptable recovery range is oscillated between 50 and 60% up to 130%. Taking into account that both, analysed low-mass PBDEs and the organic solvent of reference standard solution, are characterised by very low solubility in water, the obtained values of recovery rates might be considered as sufficient. As for the tap water, the recovery value of PBDE-47 might be at quite good level, but in a case of PBDE-99 the result is very hard to acceptance. Probably, it might be caused by the presence of chemical compounds that were used to purified and enrich the tap water. Following the data shown in Fig. 8, it might be observed a similar relationship in the recovery values for studied PBDEs determined in spiked deionised as well as the tap water (lower recovery values of PBDE-99, then PBDE-47). One of the explanations of this phenomenon might be the presence of trihalomethanes (THMs) that occur in the tap water and

might be present even in a distilled water (mainly chloroform). These compounds are generally formed as a by-products during the drinking water disinfection process with the use of chlorine (Pavón et al., 2008; Chary and Fernandez-Alba, 2012). For this reason, considering THMs chemical structure, their chemical activity, as well as their content level (these compounds might occur in drinking and tap waters from ng up to µg per litre), it is possible that they might interact with the specific binding sites. As a consequence, their presence and activity might lead to deactivation/occupation of binding sites and hinder or limit the ability to selectivity bond the target analytes in MIP material structure. Additionally, it might be assumed that THMs might affect the chemical structure of PBDE-99 and be reason of its debromination process. Nevertheless, this hypothesis might be the general issue of some future studies about the impact of selected chemical compounds on the debromination process in PBDEs as well as the possible deactivation/occupation of binding sites by THMs. In general, based on the obtained research results on selected spiked environmental samples, it might be deduced that developed DMMIP might be considered as a potential magnetic sorption material in the field of selective recognition of low-mass PBDEs in aquatic environmental samples. Following the sufficient selective sorption abilities, synthesised DMMIP might be employed as an alternative tool in the isolation and/or preconcentration process of low-mass PBDEs from the aquatic medium.

#### 4. Conclusions and future perspectives

In the present paper, 4,4'- dihydroxydiphenyl ether as a dummy-template based core-shell structured MMIP was successfully synthesised employing surface molecular imprinting technology. The physico-chemical properties and morphological surface of prepared DMMIP and its comparable MNIP were characterised and described with the use of several techniques such as FT-IR, SEM, TGA, BET and BJH. In addition, performed experiments give a possibility to describe and assess the

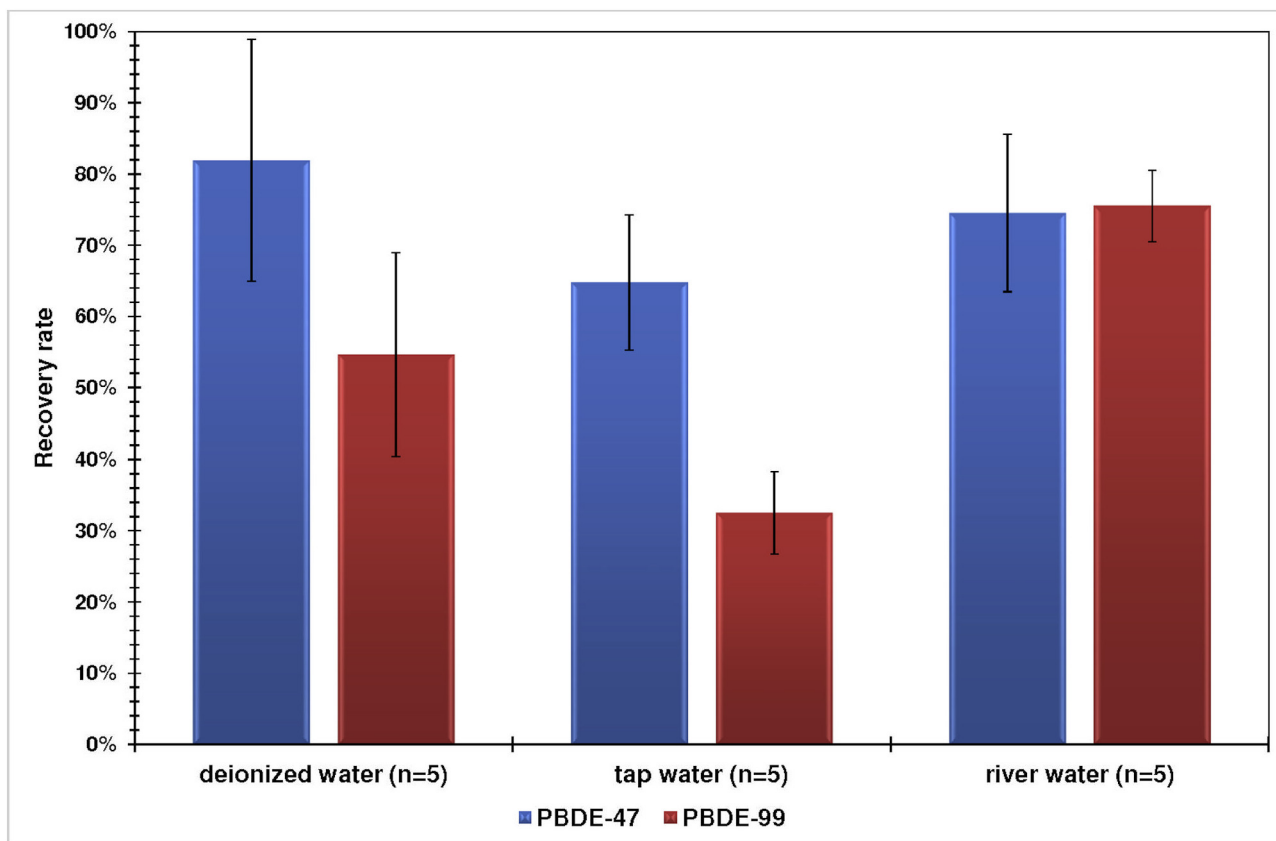


Fig. 8. The average values of recovery rates of determined low-mass PBDEs measured spiked aquatic mediums with the use of prepared DMMIP at the sample preparation process.

binding capabilities, selectivity, recovery as well as potential field of application of prepared magnetic sorption material. Considering the results of static and kinetic sorption abilities as well as the values of IF, it might be concluded that the thin film of the imprinted polymer which was immobilized on the surface of magnetic core was characterised by the presence of specific binding centres/cavities. The results of performed research give a reason to conclude that prepared DMMIP nanoparticles might be employed as a convenient analytical tool for isolation and/or preconcentration of low-mass PBDEs from aquatic medium. Considering the obtained research results, especially associated with the recovery values of determined low-mass PBDEs from studied samples, it might be concluded that developed DMMIP might be suitable for their selective recognition from environmental water samples. However, in the near future some additional and detailed research should be conducted to study and explain the potential impact on binding abilities of prepared magnetic MIP of a different groups of chemical compounds that occur in the aquatic environment, such as mentioned earlier THMs, polychlorinated biphenyls (PCBs), pesticides and particulate matter. Additionally, it was observed that some differences between sorption abilities of studied low-mass PBDEs might result from a difference in solubility, chemical structure and number of bromines as well as the fact that measured SVOCs might be regularly adsorbed on the surface of pore materials – low-mass PBDEs might be bound by the applied DMMIP not only by the specific recognition sites, but also following the conventional (standard) physicochemical adsorption. However, despite the fact that recovery values and the sorption abilities might be considered as adequate and satisfactory, in future research some slightly modifications should be considered. The adjustments might be introduced to the preparation process to obtain such magnetic MIP nanoparticles which will be able to selectively collect more analytes from PBDE group and to increase the availability of binding sites which successfully increase the recovery values and enriching factor. In addition, in future research associated with the determination of low-mass PBDEs in aquatic mediums, the presence and impact of other chemical compounds on the debromination process should be discussed. Moreover, in further more developed studies the internal standard technique (ISTD) should be considered at the stage of final determination of selected low-mass PBDEs as well as during the recovery studies. However, the potential chemical compound that might be proposed as an internal standard should not interfere the target analytes from reaching and accessing the binding sites (occupy characteristic cavities in the polymer structure).

Future research should also be broadened by performing ecotoxicology tests, as well as by the assessment of the “greenness” of both the analytical procedure and the MIP preparation process. This is of particular importance when evaluating the MIP synthesis – the use of solvents, reagents, specific chemicals as target molecules or structural analogues, and the use of laboratory equipment. As previously mentioned, and highlighted in most papers on the use of MIPs, the final product of polymerisation, i.e. the solid imprinted polymer, is generally characterised by thermal, mechanical and chemical stability, and the possibility to re-use the sorption material (Marć et al., 2018a). Additionally, it meets several of the requirements stipulated by the screening SIGNIFICANCE mnemonic technique, especially in a case of increasing the efficiency and the selectivity of the extraction process as well as decreasing the LOD and LOQ values of the entire analytical procedure (Gałaszka et al., 2013). For this reason, from the users perspective, MIPs can be considered “green” and low-toxic materials. Furthermore, there are several procedures and computer modelling solutions which can be used to estimate and visualize the green aspect or environmental impact of the employed/developed analytical protocol. These include the National Environmental Methods Index (NEMI labelling); MultiCriteria Decision Aid or Analysis (MCDA), self-organizing maps (SOM), Technique for Order Preference by Similarity to the Ideal Solution (TOPSIS); analytical Eco-scale; Green Analytical Procedure Index (GAPI) technique;

Gibbs triangle projection, as well as the combinations of the aforementioned tools (Astel, 2007; Behzadian et al., 2012; Soltani et al., 2015; Tobiszewski et al., 2015; Płotka-Wasyłka, 2018; Marć et al., 2020). The GAPI analysis was used to assess the screening semi-quantitative information about the assessment of “green” character of the applied analytical procedure for the determination of low-mass PBDEs in environmental water samples using developed DMMIP (Fig. 9). In brief, by analyzing the GAPI graph in Fig. 9 it might be noticed that a “green” solution might be found in nearly every stage of the analytical procedure. Since the use of core-shell magnetic imprinted polymers in the sample preparation process requires a very small amount of solvents, low energy expenditure and the sample preparation itself is relatively short and straightforward, they might be considered “green” extraction materials. As for the last part of the graph (the right-most pentagon) which is mainly associated with the use of stationary devices used for the final determination of analytes and waste recirculation, it is very difficult to substitute these with any “greener” solutions. This is mostly due to the use of GC-MSD (and the associated energy use for a single analysis), as well as to the use of isooctane for the low-mass PBDEs extraction.

In future studies, the assessment of the “green” aspect and ecotoxicology should be performed for each particular polymerisation technique used to obtain the desired imprinted polymer. Such kind of studies should enclose a detailed database of the most commonly used functional monomers, porogens/solvents, cross-linking agents as well as some additional and specific types of reagents used in the particular polymerisation technique. Then, considering their physicochemical properties, economic factors, and the laboratory safety aspects, the application of certain statistical calculations might yield preliminary information about the optimal reagents configuration – the optimal solution from the ecological and environmental safety point of view. However, it should be born in mind that the estimated, theoretically optimal solution might not produce desired results during the MIP preparation process due to the low efficiency of synthesis and high costs of reagents and laboratory equipment. Nevertheless, in the near future, such kind of modelling and statistical studies should be performed to narrow the spectrum of reagents (mainly functional monomers and solvents) employed during imprinted polymers polymerisation process. A recent, helpful solution when developing new types of specific imprinted materials (regardless of the employed polymerisation technique) is to introduce to the laboratory practice computational molecular modelling employed with the use of appropriate software. The application of ab-initio or semi-empirical computational techniques facilitates the reduction of the number of syntheses carried out and enables the selection of the optimal configuration of the reaction mixture containing the template molecules, functional monomers and the solvent/porogen solution (Marć et al., 2018a). For this reason, the implementation of

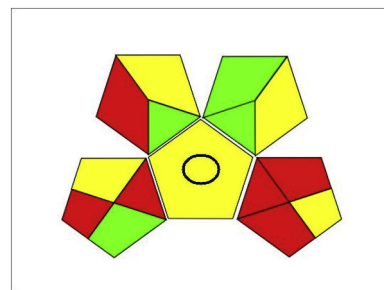


**Fig. 9.** The screening GAPI diagram acquired for the described analytical procedure with the use of prepared DMMIP at the stage of isolation and preconcentration of analytes dedicated for low-mass PBDEs determination in environmental water samples. Green colour – the green aspects; yellow colour - moderate green aspect; red colour – the minimal green aspect of selected analytical procedure stage (Płotka-Wasyłka, 2018). (For interpretation of the references to colour in this figure legend, the reader is referred to the web version of this article.)

computational molecular modelling at the initial stage of MIPs development process may result in synthesis meeting the requirements of “greenness” and significantly less adversely affect the environment (less waste). On the other hand, the selection of the polymerisation technique has the greatest impact on the number of synthesis steps (single step or multistep preparation process), the shape and the dimensions of obtained MIP particles, and their potential field of application. Because of this, the “greenness” and ecotoxicology assessment of the MIPs preparation process should be performed and evaluated separately for each polymerisation technique. Therefore, there is no ideal and universal solution to the issue of evaluating the development of new types of MIPs, and so the matter remains open and might be the basis for future research.

Supplementary data to this article can be found online at <https://doi.org/10.1016/j.scitotenv.2020.138151>.

### CRedit authorship contribution statement

**Mariusz Marć:** Conceptualization, Methodology, Validation, Formal analysis, Investigation, Resources, Writing - original draft, Writing - review & editing, Project administration, Funding acquisition. **Piotr Paweł Wiczorek:** Writing - review & editing, Supervision.

### Acknowledgements

The scientific work was financial supported by the National Science Centre, Poland, through the FUGA 5 internship project; scientific project number 2016/20/S/ST4/00151.

Mariusz Marć would like to thank Dr. Jacek Ryl and Dr. Krzysztof Formela for their valuable scientific contribution.

Mariusz Marć would like to thank Professor Bożena Zabiegała and Dr. Marek Tobiszewski for scientific support and fruitful discussion during the realization of the following paper.

### Declaration of competing interest

The authors declare that they have no conflict of interest.

### References

- Alexander, C., Andersson, H.S., Andersson, L.I., Ansell, R.J., Kirsch, N., Nicholls, I.A., O'Mahony, J., Whitcombe, M.J., 2006. Molecular imprinting science and technology: a survey of the literature for the years up to and including. *J. Mol. Recognit.* 19, 106–180.
- Alves, M.N., Miró, M., Breadmore, M.C., Macka, M., 2019. Trends in analytical separations of magnetic (nano)particles. *Trends Anal. Chem.* 114, 89–97.
- Ansari, S., 2017. Application of magnetic molecularly imprinted polymer as a versatile and highly selective tool in food and environmental analysis: recent developments and trends. *Trends Anal. Chem.* 90, 89–106.
- Ansari, S., Karimi, M., 2017. Novel developments and trends of analytical methods for drug analysis in biological and environmental samples by molecularly imprinted polymers. *Trends Anal. Chem.* 89, 146–162.
- Araghi, S.H., Entezari, M.H., 2015. Amino-functionalized silica magnetite nanoparticles for the simultaneous removal of pollutants from aqueous solution. *Appl. Surf. Sci.* 333, 68–77.
- Astel, A., 2007. Chemometrics based on fuzzy logic principles in environmental studies. *Talanta* 72, 1–12.
- Bayat, A., Shakourian-Fard, M., Ehyaei, N., Hashemi, M.M., 2014. A magnetic supported iron complex for selective oxidation of sulfides to sulfoxides using 30% hydrogen peroxide at room temperature. *RSC Adv.* 4, 44274–44281.
- Behzadian, M., Khanmohammadi Otagh Sara, S., Yazdani, M., Ignatius, J., 2012. A state-of-the-art survey of TOPSIS applications. *Expert Syst. Appl.* 39, 13051–13069.
- Berton, P., Lana, N.B., Ríos, J.M., García-Reyes, J.F., Altamirano, J.C., 2016. State of the art of environmentally friendly sample preparation approaches for determination of PBDEs and metabolites in environmental and biological samples: a critical review. *Anal. Chim. Acta* 905, 24–41.
- Chang, L., Chen, S., Li, X., 2012. Synthesis and properties of core-shell magnetic molecularly imprinted polymers. *Appl. Surf. Sci.* 258, 6660–6664.
- Chary, N.S., Fernandez-Alba, A.R., 2012. Determination of volatile organic compounds in drinking and environmental waters. *Trends Anal. Chem.* 32, 60–75.
- Cheong, W.J., Yang, S.H., Ali, F., 2013. Molecular imprinted polymers for separation science: a review of reviews. *J. Sep. Sci.* 36, 609–628.
- Choo, G., Kim, D.H., Kim, U.J., Lee, I.S., Oh, J.E., 2018. PBDEs and their structural analogues in marine environments: fate and expected formation mechanisms compared with diverse environments. *J. Hazard. Mater.* 343, 116–124.
- Demirci, B., Bereli, N., Ashlyuce, S., Baydemir, G., Denizli, A., 2017. Protein C recognition by ion-coordinated imprinted monolithic cryogels. *J. Sep. Sci.* 40, 1610–1620.
- Dinc, M., Esen, C., Mizaikoff, B., 2019. Recent advances on core-shell magnetic molecularly imprinted polymers for biomacromolecules. *Trends Anal. Chem.* 114, 202–2017.
- Gai, Q.Q., Qu, F., Liu, Z.J., Dai, R.J., Zhang, Y.K., 2010. Superparamagnetic lysozyme surface-imprinted polymer prepared by atom transfer radical polymerization and its application for protein separation. *J. Chromatogr. A* 1217, 5035–5042.
- Galuszka, A., Migaszewski, Z., Namieśnik, J., 2013. The 12 principles of green analytical chemistry and the SIGNIFICANCE mnemonic of green analytical practices. *Trends Anal. Chem.* 50, 78–84.
- Gao, D., Wang, D.D., Fu, Q.F., Wang, L.J., Zhang, K.L., Yang, F.Q., Xi, Z.N., 2018. Preparation and evaluation of magnetic molecularly imprinted polymers for the specific enrichment of phloridzin. *Talanta* 178, 299–307.
- Ge, Y., Butler, B., Mirza, F., Habib-Ullah, S., Fei, D., 2013. Smart molecularly imprinted polymers: recent developments and applications. *Macromol. Rapid Commun.* 34, 903–915.
- Gul, S., Shah, N., Arain, M.B., Rahmana, N., Rehan, T., Ul-Islam, M., Ullah, M.W., Yang, G., 2019. Fabrication of magnetic core shell particles coated with phenylalanine imprinted polymer. *Polym. Test.* 75, 262–269.
- Guo, L., Ma, X., Xie, X., Huang, R., Zhang, M., Li, J., Zeng, G., Fan, Y., 2019. Preparation of dual-dummy-template molecularly imprinted polymers coated magnetic graphene oxide for separation and enrichment of phthalate esters in water. *Chem. Eng. J.* 361, 245–255.
- Gustavsson, J., Ahrens, L., Nguyen, M.A., Josefsson, S., Wiberg, K., 2017. Development and comparison of gas chromatography-mass spectrometry techniques for analysis of flame retardants. *J. Chromatogr. A* 1481, 116–126.
- Hashemi, M., Nazari, Z., Noshirvani, N., 2017. Synthesis of chitosan based magnetic molecularly imprinted polymers for selective separation and spectrophotometric determination of histamine in tuna fish. *Carbohydr. Polym.* 177, 306–314.
- He, J., Huang, M., Wang, D., Zhang, Z., Li, G., 2014. Magnetic separation techniques in sample preparation for biological analysis: a review. *J. Pharm. Biomed. Anal.* 101, 84–101.
- He, Y., Zhao, F., Zhang, C., Abd El-Aty, A.M., Baranenko, D.A., Hacimüftüoğlu, A., She, Y., 2019. Assessment of magnetic core-shell mesoporous molecularly imprinted polymers for selective recognition of triazoles residual levels in cucumber. *J. Chromatogr. B* 1132, 121811.
- Hu, Y., Li, J., Zhang, Z., Zhang, H., Luo, L., Yao, S., 2011. Imprinted sol-gel electrochemical sensor for the determination of benzylpenicillin based on Fe<sub>3</sub>O<sub>4</sub>@SiO<sub>2</sub>/multi-walled carbon nanotubes-chitosans nanocomposite film modified carbon electrode. *Anal. Chim. Acta* 698, 61–68.
- Khan, T.A., Chaudhry, S.A., Ali, I., 2015. Equilibrium uptake, isotherm and kinetic studies of Cd(II) adsorption onto iron oxide activated red mud from aqueous solution. *J. Mol. Liq.* 202, 165–175.
- Khan, S., Hussain, S., Wong, A., Foguel, M.V., Gonçalves, L.M., Gurgo, M.I.P., Sotomayor, M.P.T., 2018. Synthesis and characterization of magnetic-molecularly imprinted polymers for the HPLC-UV analysis of ametryn. *React. Funct. Polym.* 122, 175–182.
- Komolafe, O., Bowler, B., Dolfing, J., Mrozik, W., Davenport, R.J., 2019. Quantification of polybrominated diphenyl ether (PBDE) congeners in wastewater by gas chromatography with electron capture detector (GC-ECD). *Anal. Methods* 11, 3474–3482.
- Król, S., Zabiegała, B., Namieśnik, J., 2012. PBDEs in environmental samples: sampling and analysis. *Talanta* 93, 1–17.
- Król, S., Namieśnik, J., Zabiegała, B., 2014. Occurrence and levels of polybrominated diphenyl ethers (PBDEs) in house dust and hair samples from northern Poland; an assessment of human exposure. *Chemosphere* 110, 91–96.
- Kubo, T., Otsuka, K., 2016. Recent progress in molecularly imprinted media by new preparation concepts and methodological approaches for selective separation of targeting compounds. *Trends Anal. Chem.* 81, 102–109.
- Marć, M., Wiczorek, P.P., 2019. Application potential of dummy molecularly imprinted polymers as solid-phase extraction sorbents for determination of low-mass polybrominated diphenyl ethers in soil and sediment samples. *Microchem. J.* 144, 461–468.
- Marć, M., Kupka, T., Wiczorek, P.P., Namieśnik, J., 2018a. Computational modeling of molecularly imprinted polymers as a green approach to the development of novel analytical sorbents. *Trends Anal. Chem.* 98, 64–78.
- Marć, M., Panuszko, A., Namieśnik, J., Wiczorek, P.P., 2018b. Preparation and characterization of dummy-template molecularly imprinted polymers as potential sorbents for the recognition of selected polybrominated diphenyl ethers. *Anal. Chim. Acta* 1030, 77–95.
- Marć, M., Bystrzanowska, M., Tobiszewski, M., 2020. Exploratory analysis and ranking of analytical procedures for short-chain chlorinated paraffins determination in environmental solid samples. *Sci. Total Environ.* 711, 134665.
- Moein, M.M., Rehim, A.A., Abdel-Rehim, M., 2019. Recent applications of molecularly imprinted sol-gel methodology in sample preparation. *Molecules* 24, 2889.
- Niu, M., Pham-Huy, C., He, H., 2016. Core-shell nanoparticles coated with molecularly imprinted polymers: a review. *Microchim. Acta* 183, 2677–2695.
- Pan, Y., Chen, J., Zhou, H., Tam, N.F.T., 2018. Changes in microbial community during removal of BDE-153 in four types of aquatic sediments. *Sci. Total Environ.* 613–614, 644–652.
- Pavón, J.L.P., Martín, S.H., Pinto, C.G., Cordero, B.M., 2008. Determination of trihalomethanes in water samples: a review. *Anal. Chim. Acta* 629, 6–23.
- Pietrofi, J.W., Małagocki, P., 2017. Quantification of polybrominated diphenyl ethers (PBDEs) in food. A review. *Talanta* 167, 411–427.



- Plotka-Wasyłka, J., 2018. A new tool for the evaluation of the analytical procedure: Green Analytical Procedure Index. *Talanta* 181, 204–209.
- Pountney, A., Filby, A.L., Thomas, G.O., Simpson, V.R., Chadwick, E.A., Stevens, J.R., Tyler, C.R., 2015. High liver content of polybrominated diphenyl ether (PBDE) in otters (*Lutra lutra*) from England and Wales. *Chemosphere* 118, 81–86.
- Pupin, R.R., Foguel, M.V., Gonçalves, L.M., Sotomayor, M.P.T., 2020. Magnetic molecularly imprinted polymers obtained by photopolymerization for selective recognition of penicillin G. *J. Appl. Polym. Sci.* 137, 48496.
- Rocio-Bautista, P., Gonzalez-Hernandez, P., Pino, V., Pasan, J., Afonso, A.M., 2017. Metal-organic frameworks as novel sorbents in dispersive-based microextraction approaches. *Trends Anal. Chem.* 90, 114–134.
- Seraj, S., Lotfollahi, M.N., Nematollahzadeh, A., 2020. Synthesis and sorption properties of heparin imprinted zeolite beta/polydopamine composite nanoparticles. *React. Funct. Polym.* 147, 104462.
- Soltani, A., Hewage, K., Reza, B., Sadiq, R., 2015. Multiple stakeholders in multi-criteria decision-making in the context of municipal solid waste management: a review. *Waste Manag.* 35, 318–328.
- Speltini, A., Scalabrini, A., Maraschi, F., Sturini, M., Profumo, A., 2017. Newest applications of molecularly imprinted polymers for extraction of contaminants from environmental and food matrices: a review. *Anal. Chim. Acta* 974, 1–26.
- Stapleton, H.M., 2006. Instrumental methods and challenges in quantifying polybrominated diphenyl ethers in environmental extracts: a review. *Anal. Bioanal. Chem.* 386, 807–817.
- Stockholm-Convention, 2010. The 9 new POPs. Proceedings of the Fourth Meeting of an Introduction to the Nine Chemicals Added to the Stockholm Convention by the Conference of the Parties.
- Tobiszewski, M., Marć, M., Gałuszka, A., Namieśnik, J., 2015. Green chemistry metrics with special reference to green analytical chemistry. *Molecules* 20, 10928–10946.
- Vasapollo, G., Del Sole, R., Mergola, L., Lazzoi, M.R., Scardino, A., Scorrano, S., Mele, G., 2011. Molecularly imprinted polymers: present and future prospective. *Int. J. Mol. Sci.* 12, 5908–5945.
- Wang, X.T., Chen, L., Wang, X.K., Zhang, Y., Zhou, J., Xu, S.Y., Sun, Y.F., Wu, M.H., 2015. Occurrence, profiles, and ecological risks of polybrominated diphenyl ethers (PBDEs) in river sediments of Shanghai, China. *Chemosphere* 133, 22–30.
- Watanabe, I., Sakai, S., 2003. Environmental release and behavior of brominated flame retardants. *Environ. Int.* 29, 665–682.
- Wei, M., Yan, X., Liu, S., Liu, Y., 2018. Preparation and evaluation of superparamagnetic core-shell dummy molecularly imprinted polymer for recognition and extraction of organophosphorus pesticide. *J. Mater. Sci.* 53, 4897–4912.
- de Wit, C.A., Herzke, D., Vorkamp, K., 2010. Brominated flame retardants in the Arctic environment – trends and new candidates. *Sci. Total Environ.* 408, 2885–2918.
- Wu, M., Fan, Y., Li, J., Lu, D., Guo, Y., Xie, L., Wu, Y., 2019. Vinyl phosphate-functionalized, magnetic, molecularly-imprinted polymeric microspheres' enrichment and carbon dots' fluorescence-detection of Organophosphorus pesticide residues. *Polymers* 11, 1770.
- Xie, X., Chen, L., Pan, Y., Wang, S., 2015. Synthesis of magnetic molecularly imprinted polymers by reversible addition fragmentation chain transfer strategy and its application in the Sudan dyes residue analysis. *J. Chromatogr. A* 1405, 32–39.
- Xu, L., Pan, J., Dai, J., Li, X., Hang, H., Cao, Z., Yan, Y., 2012. Preparation of thermal responsive magnetic molecularly imprinted polymers for selective removal of antibiotics from aqueous solution. *J. Hazard. Mater.* 233–234, 48–56.
- Xu, J., Ju, C., Sheng, J., Wang, F., Zhang, Q., Sun, G., Sun, M., 2013. Synthesis and characterization of magnetic nanoparticles and its application in lipase immobilization. *Bull. Kor. Chem. Soc.* 34, 2408–2412.
- Yan, Y., Li, Y., Ma, M., Ma, W., Cheng, X., Xu, K., 2018. Effects of coexisting BDE-47 on the migration and biodegradation of BDE-99 in river-based aquifer media recharged with reclaimed water. *Environ. Sci. Pollut. Res.* 25, 5140–5153.
- Zhang, Z., Luo, L., Cai, R., Chen, H., 2013. A sensitive and selective molecularly imprinted sensor combined with magnetic molecularly imprinted solid phase extraction for determination of dibutylphthalate. *Biosens. Bioelectron.* 49, 367–373.
- Zhang, Z., Niu, D., Li, Y., Shi, J., 2018. Magnetic, core-shell structured and surface molecularly imprinted polymers for the rapid and selective recognition of salicylic acid from aqueous solutions. *Appl. Surf. Sci.* 435, 178–186.
- Zuo, H.G., Zhu, J.X., Zhan, C.R., Shi, L., Xing, M., Guo, P., Ding, Y., Yang, H., 2015. Preparation of malathion MIP-SPE and its application in environmental analysis. *Environ. Monit. Assess.* 187, 394.

